MIT
SEA
GRANT
PROGRAM

MARINE ENVIRONMENT EFFECTS ON FATIGUE CRACK PROPAGATION IN GRP LAMINATES FOR HULL CONSTRUCTION

by

Robert P. Demchik
John F. Mandell
Frederick J. McGarry

Massachusetts Institute of Technology

Cambridge, Massachusetts 02139

Report No. MITSG 73-16
November 30, 1973

MARINE ENVIRONMENT EFFECTS ON FATIGUE CRACK PROPAGATION IN GRP LAMINATES FOR HULL CONSTRUCTION

by

Robert P. Demchik
John F. Mandell
Frederick J. McGarry

MITSG73-16
Index #73-316-Cfo

TABLE OF CONTENTS

ABSTRACT

The effects of a salt water environment on the fatigue properties of a particular GRP laminate construction, suitable for hull construction, are examined experimentally. The experimental S-N curves for both an air and a salt water environment are given and comparison of the two curves shows a general, but moderate, decrease in the fatigue life of the material in a salt water environment.

A recently developed theory for fatigue crack growth in composite materials is used as the basis of comparison of experimental data obtained for the relationship between fatigue crack growth rate and stress intensity factor. The theory is confirmed for the specific material used in this study when a linear approximation to the S-N curves is made. Further, the mechanism of fatigue crack growth is confirmed as one of the ligament advance.

Additional experimental work to refine the theory is recommended.

I. INTRODUCTION

The development of glass fiber-reinforced plastics has advanced to a point where these materials are now considered serious competitors for the more standard structural materials such as wood, metals and concrete for many applications. The recent construction of a 153-foot minehunter, HMS Wilton, by the British (1) is witness to the feasibility of building larger, sea-going vessels of reinforced plastics. What problems may develop after a significant service life remain to be seen. Meanwhile, investigations must continue that will add to the store of knowledge about the properties of these materials.

A substantial amount of investigation has been conducted into the fracture toughness properties of various glass-plastic composites. Emphasis in many studies has been on determining whether the principles of fracture mechanics as developed for homogeneous materials, and widely applied to metals, might be applicable to composites. In general, it seems to have been established that such is, indeed, the case with some modifications (2).

One aspect of the fracture of glass-reinforced composites that has received little attention to date is the fatigue life. Fatigue fracture is defined as the failure of a material under repeated loading. The higher the cyclical stress, the lower will be the number of cycles endured to failure. The fatigue characteristics of a material are

commonly displayed in the form of a Wohler, or S-N, curve which gives the number of cycles to failure at a given nominal stress. Ferrous metals exhibit a fatigue limit defined simply as a stress below which the fatigue life is considered infinite (3).

Fatigue properties must be adequately defined in order to insure proper and safe design of a structure - particularly a structure that can be expected to see repeated loadings during its lifetime. Structural components in the vicinity of machinery foundations or in other areas of considerable vibrations are practical examples of components that might be subjected to several millions of cycles of stress in a relatively short period of time. For a vibration frequency of only 6 cycles per second, such a component will undergo over one million reversals of stress in a period of two days.

This investigation attempts to take a step in the direction of defining the fatigue properties of a glass-reinforced plastic by experimentally determining the fatigue characteristics of a particular laminate configuration which might be used in the construction of a ship hull. More specifically, the goals of this study are to;

1. define the S-N curve for a hull construction type of composite,

2. determine the fatigue crack propagation rate as a function of stress intensity factor for the same material,

3. determine the effect, if any, of a salt water environment on both the S-N curve and the fatigue crack propagation rate, and

4. develop a means of predicting the crack propagation rate from the data contained in the S-N curve.

A study of the fatigue properties of crossplied Scotchply (a high performance, high volume fraction, pre-preg, uni-directional ply, glass-reinforced epoxy) laminates by Mandell and Meier (4) showed that, for that material, crack growth rate varied approximately with the eleventh power of stress intensity factor. In Scotchply it was noted that a fatigue crack grows by propagating rapidly through a discrete "ligament" of the composite and then remaining at one position for many cycles before propagating through another ligament. (This is in contrast to the case for metals in which a fatigue crack grows a minute amount on every cycle.) A simple theoretical prediction of the crack growth rate from the fracture toughness, ultimate tensile strength and S-N curve for the unnotched material yielded an exponential relationship between crack growth rate and stress intensity factor which was in good agreement with the experimental data.

The composite chosen for the present study is considerably more complex than Scotchply in physical make-up. However, the same basic method is employed to analyze the experimental data and to display the results as was used

in the Mandell-Meier study. The purpose of this approach is to attempt to determine if the proposed theory might be more widely applicable than to Scotchply alone. An unnotched, dogbone-shaped specimen is used to define the S-N curves for both the air and salt water environments. A specially-designed, "index card" specimen is used for the determination of crack propagation rate in both the air and salt water environments. The index card is also analyzed for K-calibration and the dogbone specimen is used to determine Young's Modulus.

II. MATERIALS

In fabricating the specimens for this investigation, an attempt was made to simulate an actual production method that might be used in constructing a medium-sized boat of the same material. Details of the fabrication procedure and particulars of the materials can be found in Appendix C.

The composite plates were prepared in 30" by 38" sections using alternate layers of chopped fiber, random mat glass and woven roving glass fabric in a matrix of polyester resin. Methyl ethyl ketone peroxide was used as the curing catalyst.

In the early stages of the experimental portion of the work, a laminate consisting of three layers of chopped mat and two layers of woven roving was used. The specimen chosen for determining crack propagation rate was a 3" by 10" double edge-notched specimen. This specimen type had to be abandoned when it was found that the crack always propagated too rapidly to permit measurement of the rate. A 3" by 5", index card specimen was substituted but was also found to be unsuitable because it buckled under load. The configuration was then changed to one requiring five layers of chopped mat and four layers of woven roving. Both the notched and unnotched specimens of this construction proved satisfactory. A volume fraction of about 30% was desired and was roughly controlled by controlling plate thickness during fabrication. Burn tests conducted on four

representative one-inch squares from the three plates revealed an average actual volume fraction of 30.45%.

The plates were made using a standard, hand-lay-up technique and were cured in air with no heat or pressure applied. The plates were then cut into specimens and the specimens were machined to final dimensions as described in Appendix C. The geometry of both specimens is shown in Figure 2.

The salt water used for both the presoak bath and the testing environment was manufactured as needed using distilled water and 3% by weight of sodium chloride (C.P. granular - Mallinckrodt Chemical Works). The solution was usually made in batches consisting of 4000 ml of distilled water and 124 grams of Na Cl.

III. EXPERIMENTAL PROCEDURE

A fatigue stress cycle is completely defined by specifying any two of the four possible parameters of the cycle- the maximum stress, the minimum stress, the mean stress and the stress range. The Instron Model 1211 Dynamic Cycler, which was to be used for all fatigue testing, permits the operator to pre-set the mean load and any one of the remaining three parameters in terms of loads - the resulting stresses being determined simply by dividing the load by the cross-sectional area of the specimen. All specimens were to be tested in tension-tension stress cycles. If the minimum load were allowed to go to zero, the grip assemblies would slacken and motion of the specimen would result. Therefore, it was decided that the minimum load in all stress cycles would be standardized at 80 pounds for the index card specimens and at 400 pounds for the dogbone specimens; these specific loads were chosen because they both represent 4% of the full range load scales used. The problem of specimen motion was thereby eliminated. Tables 1a and 1b give the specifications for the ten loading conditions used in the tests. The machine was set up for 2000 pounds full scale load for the index card specimens and for 10,000 pounds full scale load for the dogbone specimens. The two parameters used for controlling the tests were the mean load and the load range (the fatigue cycle was load-controlled).

In order to determine suitable load cycles for the fatigue tests, it was intended to find the ultimate load that could be sustained by each type of specimen and establish fatigue cycles in which the maximum loads were various fractions of the ultimate loads. The composite was known to be rate-sensitive and it was desired to test for ultimate load at approximately the same rate as would be achieved in the fatigue tests. Both the Instron Universal Testing Machine and the Instron Model 1211 Dynamic Cycler were used to obtain initial indications of ultimate loads. Neither of these machines, however, was capable of reaching the required rate. Therefore, actual values of ultimate loads were not determined until after fatigue tests were completed when an Instron Universal Static/Dynamic Testing Instrument Model 1250 was made available by Instron Corporation at their Canton, Massachusetts facility. Thus, the fatigue stress cycles used were based on the estimates of ultimate loads found from testing in air on the IUTM and the Model 1211. The estimated ultimate loads were 9200 pounds for the unnotched specimens and 1200 pounds for the notched specimens. The same loading conditions were applied to tests in both air and salt water.

Preliminary fatigue testing to determine practical limits on stress cycles indicated that for a stress cycle in which the maximum load was less than about 40% of the estimated ultimate load the time required to test to failure was excessive (on the order of 10^7 cycles). This

resulted from the fact that all testing was to be done at a frequency of 6 cycles per second. At higher frequencies, the material heated up noticeably and at sufficiently high frequencies the material would actually burn because of internal friction. Similarly, for a stress cycle in which the maximum load was greater than about 80% of the estimated ultimate load the specimen failed so rapidly that an accurate determination of the number of cycles to failure was virtually impossible. Based upon these preliminary tests, fatigue stress cycles were chosen in which the maximum loads were 40%, 50%, 60%, 70% and 80% of the estimated ultimate loads. The corresponding values of maximum load ranged from 3680 to 7360 pounds for the unnotched specimens and from 480 to 960 pounds for the notched specimens.

A description of all major apparatus used can be found in Appendix D. The set-up procedure for all tests was basically the same. In the case of the tests in salt water, the salt water containment system was first installed on the Dynamic Cycler. The salt water box was filled with sodium chloride solution to a level sufficient to completely cover the specimen. In anticipation of the effect of salt water on the metal parts required for gripping the specimens, all parts that would come in contact with salt water were either chrome-plated or made of brass or stainless steel. As a result of wearing and chipping of the chrome plate, however, substantial corrosion of the base metal (low-carbon steel) took place - particularly in the

later tests. This was manifested in the form of rather profuse amounts of a rust-colored precipitate. The amount of this precipitate was kept to a minimum by changing the water frequently. No attempt was made to analyze the precipitate nor to determine its effect, if any, on the tests.

In preparation for each test, the Dynamic Cycler was zeroed, balanced and calibrated in accordance with the technical manual. The stress cycle was set by adjusting the PRE-LOAD dial to the appropriate mean load and by placing the FUNCTION switch to the Δ-LOAD position and adjusting the dial to the appropriate load range. The cycler was turned on and the frequency was checked to insure that the Hz meter always showed 7 Hz. (This reading on the Hz meter corresponded to an actual frequency of 5.93 Hz as determined from timing the frequency counter over about 500,000 cycles on several, separate occasions.) The ram position required to maintain the load cycle was controlled automatically by depressing the AUTO button in the STROKE CONTROL section of the panel.

Data-taking from the unnotched specimens consisted simply of noting the number of cycles to failure for each specimen. This information, together with the nominal maximum stress on the specimen, was sufficient to define the S-N curves for both the air and salt water environments. Three specimens were tested at each stress cycle for both the air and salt water environments.

The notched specimens were marked with lines perpendi-

cular to the notch at one-eighth inch intervals to facilitate determination of the location of the crack tip. The single biggest problem in the experimental work was the accurate location of the crack tip. The surface crack was not considered to be a reliable indication because significant debonding of individual fibers in the outside layers of random mat confused the appearance of the crack to such an extent that this method was discarded. The method eventually accepted resulted from a visual correlation between the location of the crack tip as indicated photo-elastically by cross-polarized light and the location as determined by cutting several specimens progressively closer to the surface crack tip until the specimens easily parted into two pieces. Comparison of the two locations of the crack tip suggested that viewing the crack through polarized light while the specimen was under load gave the crack tip location as the beginning of the dark interference band near the crack tip. Though this method was recognized as being imperfect it was employed to obtain all crack growth rate data. The accepted crack tip location is shown schematically in Figure 8.

The data-taking from the notched specimens consisted of determining the location of the crack tip as accurately as possible (considered to be to the nearest half-interval, i.e., 1/16") and recording both the crack tip location and the total number of cycles elapsed up to the time of that determination. Growth rate could then be found by dividing

the distance the crack advanced by the number of cycles required for that advance distance. A replication factor of three was again used for both the air and salt water environments.

A time schedule was established for those specimens that were to be presoaked in salt water prior to testing. The ten-day presoak period was measured from the time a specimen was inserted into the bath until the time it was installed in the Dynamic Cycler to begin testing, exclusive of the time required to perform the test. Thickness measurements and weights were taken prior to placing the specimens in the bath in order to discern whether or not any significant water absorption took place.

To determine the appropriate rate at which to test specimens for actual ultimate tensile strength, a static test was performed on one of each of the two specimen types. A large retaining nut (used to secure the salt water containment system to the Dynamic Cycler) was threaded into place and a specimen was installed. The PRE-LOAD dial was set to 400 pounds for the dogbone specimen or 80 pounds for the index card specimen (P_{min} in the respective 60% load cycles) and the pin of a dial indicator was rested on the retaining nut. The dial indicator position was adjusted so that a deflection of about 0.3 inch was indicated with the minimum load applied. The PRE-LOAD dial was then adjusted to 5520 pounds for the dogbone specimen or 720 pounds for the index card specimen (P_{max} in the respective

60% load cycles) and the change in dial indicator deflection between the two loading conditions for the two specimens was noted. Knowing this deflection and the frequency at which the fatigue tests were conducted the strain rate was determined from;

$$(2c\ \frac{\text{in}}{\text{cyc}})(f\ \frac{\text{cyc}}{\text{sec}})(60\ \frac{\text{sec}}{\text{min}}) = \text{strain rate}\ \frac{\text{in}}{\text{min}},$$

where c is the deflection change from the dial indicator.

The strain rates thus obtained were 60 in/min for the dogbone specimen and 30 in/min for the index card specimen. Using the 60% load cycles was considered to provide average strain rates for all fatigue loading conditions. Tables 2a and 2b give the data acquired from ultimate strength tests.

IV. ANALYTICAL METHOD

One of the purposes in conducting this study was to develop a means of predicting crack growth rate from information contained in the S-N curve for the material. With this in mind, the analysis was formulated in such a way that the observed variation of crack growth rate with stress intensity factor could be compared with the relationship between crack growth rate and stress intensity factor as predicted by the theory developed by Mandell and Meier for Scotchply.

The basis of the theory lies in the hypothesis that the material at the tip of a crack will fail in fatigue in accordance with the S-N curve for unnotched specimens of the same material, the fatigue life being determined by the local stress level at the crack tip. Since the material local to the crack tip must reach its local ultimate tensile strength at the same time as the stress intensity factor reaches the value of the candidate critical stress intensity factor, it can be stated that;

$$\sigma_1 = \sigma_f \frac{K_I}{K_Q} . \qquad (1)$$

The assumption of linearity between σ_1 and σ_f implied by this equation is questioned by Mandell and Meier because of the growth of the splits at the crack tip during the fatigue process. The initiation and growth of such splits have been shown to be the source of fracture toughness in

composites of this type (6). The validity of the linearity assumption might also be questioned in this instance, although the growth of vertical splits was not as evident for the material and geometry used for this investigation.

If the S-N curve for the unnotched material can be defined (or at least approximated) by a straight line, its equation can be written as;

$$\log N = \frac{\sigma_f - \sigma}{s} . \qquad (2)$$

If, then, σ_1 from equation (1) is inserted into equation (2) for σ, the result is;

$$\log N = \frac{\sigma_f}{s} \left(1 - \frac{K_I}{K_Q} \right) . \qquad (3)$$

To facilitate the prediction of crack growth rate, the assumption is made that the effect of the stress distribution beyond the crack tip is negligible. For all crack lengths, the stress immediately at the crack tip is taken as that given by equation (1) and zero stress prevails elsewhere. This assumption has the effect of neglecting any cumulative damage that may occur ahead of the crack tip. Mandell and Meier showed that , for ligament widths greater than o.oo1 inch for Scotchply, neglecting the cumulative damage effect introduced insignificant error. Additionally, only a minor difference was noted between their predicted curve neglecting cumulative damage and their curve accounting for cumulative damage over the first five ligaments ahead of the crack tip.

The final assumption is made, based on experimental observation, that the mechanism of material failure is one of ligament advance - that is, the fatigue crack advances a distance d during a very small number of cycles and then remains at the new position for many cycles before advancing by another ligament width.

With this basis for the analysis established, crack growth rate can be found by dividing the distance d by the number of cycles given by equation (3);

$$\frac{da}{dN} = \frac{d}{\exp\ 2.3\left[\frac{\sigma_f}{s}\left(1 - \frac{K_I}{K_Q}\right)\right]} . \qquad (4)$$

The important dimension d could only be found by observing the growth of the crack in the notched specimens during the fatigue tests. This task was quite difficult in the cases of both the very low and very high load cycles because of the problem of timing the observation to the very short interval when the crack propagated. Based on observations made during the tests on specimens loaded to 600, 720 and 840 pounds (P_{max}), a value of 0.125 inch was assigned to d.

In order to reduce the data for purposes of comparison with the relationship given by equation (4), two methods were employed. The first was based on the Irwin-Kies K-calibration tests (7) described in Appendix E. The stress intensity factor and crack propagation rate were evaluated within each loading cycle at each observed value

of crack length. An average of about six data points were provided by each of the notched index card specimens tested.

Boundary collocation K-calibration also has been found to be useful in applications such as this (8). Gross and Srawley developed a fitting equation to boundary collocation results (9) which gives stress intensity factor as a function of crack length, load and specimen geometry. The equation,

$$\frac{KBH^{\frac{1}{2}}}{P} = 3.46\ (\frac{a}{H} + 0.7), \qquad (5)$$

is specifically for the index card type of specimen (assuming infinite specimen length) used in this work to obtain crack growth rate data and thus might be expected to give good results. In applying equation (5), B and H were fixed by the specimen geometry. The equation then reduces to;

$$K = P(8.72\ a + 9.13). \qquad (6)$$

Values of crack length, a, and the maximum load in the cycle under which a particular specimen was fatigued, P_{max}, were inserted into equation (6) to provide values for K. The values of crack growth rate again were the rates observed during the experiments.

The candidate critical stress intensity factor, K_Q, was validated as a material property by running a K-calibration test similar to that described by Bowie (10) for symmetrically edge-cracked specimens. Three index card specimens were tested in tension at a constant strain rate (0.02 in/min). As the crack extended from the notch, the

load at every one-eighth inch interval of growth was noted. The Irwin-Kies formula was used to reduce the data. Inspection of Figure 10 shows that K_Q varies relatively little around the average value of about 17.5 ksi-in$^{\frac{1}{2}}$. The data used to plot Figure 10 are given in Table 5.

V. RESULTS

The experimental results and their comparison with theoretical behavior are displayed in Figures 12 through 15 in Appendix A. The data that produced these results are given in Tables 6 through 11 in Appendix B.

S-N Curves

The fatigue data from the unnotched specimens produced non-linear S-N curves in the cases of both air and salt water environments. For purposes of attempting to verify the Mandell-Meier theory, the linear approximations shown in Figures 12 and 13 were used. For the air environment, the approximation gave a value for σ_f of 31.0 ksi and a value for the slope, s, of 3.48 ksi per decade of cycles. In the case of the salt water environment, the linear approximation gave a value for σ_f of 27.0 ksi and a value for the slope of 3.14 ksi per decade of cycles. These values were used to plot the theoretical curves of $\frac{da}{dN}$ vs K in Figures 14 and 15.

Comparison of the S-N curves for the two different environments shows a general, but moderate, tendency toward decreased fatigue life for the salt water environment. Alternatively, for a given number of cycles, a lower stress can be withstood in salt water than in air. This is pointed out by the 10% lower value of σ_f in salt water. The percentage variation in slope between the two curves is about

equal to the percentage variation in σ_f .

Crack Propagation Rates

In Figures 14 and 15, the data for $\frac{da}{dN}$ vs K are plotted to compare with the curve given by the Mandell-Meier theory for fatigue behavior. It can be seen that substantial agreement exists between the theory and the experimental results. Because the experimental data reduced by both the Irwin-Kies and the Gross-Srawley methods gave essentially identical results, only the Irwin-Kies data points are plotted. Both the theoretical and experimental results indicate that crack growth rate is proportional to about the twelfth power of stress intensity factor, regardless of the environment. Comparison of Figures 14 and 15 also shows that the salt water environment shifts the curve and the data to the left (or up) by a constant amount along the length of the curve on the log-log plot.

General

For a given crack length within a given fatigue load cycle, reduction of the data by the Irwin-Kies formula gave precisely the same values as reduction by the Gross-Srawley formula except at very long crack lengths, where the assumption of infinite specimen length for the Gross-Srawley case was violated.

No significant increase in either thickness or weight of

the specimens presoaked in salt water was observed indicating that, at least for a ten-day presoak period, water absorption by the material was negligible.

VI. DISCUSSION OF RESULTS

Although the data obtained from the unnotched specimens did not produce linear S-N curves, very close-fitting straight lines could be passed through all of the data points except the points representing the actual ultimate tensile strengths. When these linear approximations were made, the straight lines were extrapolated to one cycle to provide values of σ_f for use in equation (4). These approximations can only be considered valid in the regions where the actual curves and the straight lines are very close. In this instance, those regions covered all of the data points other than the ultimate tensile strengths.

The fact that the S-N curves were not linear correlates with previous observations (11) in which a sharp drop-off in the S-N curve was noted. This phenomenon is especially pronounced for composites containing a polyester resin matrix. The conclusion to be drawn from the sharp drop is that the first several cycles at high loads greatly degrade the material thereby producing shorter fatigue lives than might be hoped for from simply knowing the ultimate tensile strength and expecting a linear curve.

Another factor bearing on the non-linearity of the S-N curves in this particular case is provided by closer scrutiny of the manner in which the strain rate to be used for the UTS tests was determined. The fact that a static test

was employed to determine a dynamic parameter leaves the method open to criticism. If the static test result gave a strain rate that was too high, the resulting value of UTS would be too high and some non-linearity would thus be introduced.

Unfortunately, the absence of data between the UTS and the highest stress levels at which fatigue tests were conducted precluded further definition of the true curve in this area. This was a result not only of the fact that the true UTS values were not known until after the fatigue tests were run but also of the difficulty that would be encountered in attempting to find the number of cycles in the very short fatigue lives at stress levels in the empty region. The magnitude of the void of data can be best appreciated by comparing the nominal maximum stress in the highest fatigue stress cycle (about 22,700 psi dry) with the ultimate tensile strength (about 40,000 psi dry).

In this regard, a constraint is imposed by the limited capability of the Model 1211 to achieve the preset stroke in a reasonable number of cycles. The Model 1211 is not at all suitable for measurement of fatigue life when that fatigue life is below several hundred cycles. The Model 1250 is the preferred machine for the lower cycle fatigue tests.

The wet strength retention of this material was found to be about 90%. This fits very well with data obtained on

a very similar type of composite used in a submarine fairwater (12), which also showed a wet strength retention of about 90% after eleven years of marine service life.

Because of the close agreement between the Irwin-Kies and the boundary collocation K-calibrations, the Irwin-Kies method is seen to be a useful tool in experiments utilizing an index card type of specimen.

In view of the close agreement between the experimental data and the Mandell-Meier theory, it appears that the theory is confirmed for this material. Indeed, the temptation is great to say that the theory is widely applicable to a broad range of composite constructions since Scotchply and the material used in this study differ so greatly. It is important to note that confirmation of the theory also serves to justify the assumptions made and to confirm the mechanism as one of ligament advance.

VII. CONCLUSIONS

1. The material tested produced non-linear S-N curves in both air and salt water environments. This should be expected because a polyester resin matrix was used. Because of the possibility of an erroneous method having been employed to determine ultimate tensile strength, the full reason for the non-linearity is left unexplained. It is possible that the S-N curves would, in fact, have been more nearly linear if a lower strain rate were used in the UTS tests.

2. Salt water decreases the fatigue life of the material by variable amounts depending on the stress cycle. The effect is minimized at low stress levels.

3. The Irwin-Kies K-calibration method is a simple but useful tool for use in studies involving fracture toughness and fatigue properties.

4. The Model 1211 Dynamic Cycler is not suitable for fatigue testing at stress levels close to the ultimate tensile strength of the material. The faster response of the Model 1250 Static/Dynamic Testing Instrument makes it the preferred testing machine for low cycle fatigue.

5. The Mandell-Meier theory of fatigue crack propagation is a viable theory for application to a wide range of composite materials. Crack growth by ligament advance appears to be a valid mechanism for the fatigue behavior.

VIII. RECOMMENDATIONS

The work contained in this study was intended only as a preliminary step in developing a viable theoretical approach to the fatigue performance of glass-plastic composites. The fact that the experimental results of this study seem to confirm the pioneering work of Mandell and Meier is indeed encouraging. That very confirmation, however, carries with it the need for more and expanded testing programs conceived with the idea of attacking the theory from a critical viewpoint in order to either firmly refute it or to further refine it until it becomes widely accepted and used.

Future programs in fatigue testing of composites, particularly those of complex configurations, should provide for testing at a sufficient number of stress levels to specify the S-N curve without ambiguity. The Wohler diagram is the starting point for all fatigue study and should be undeniably well-defined. Where time permits, very low stress cycles should be included to determine whether or not the material exhibits an endurance limit.

Research is needed into methods that would be suitable for accurate determination of the crack tip location in those materials where uncertainty may exist. Methods that might be considered are visual (including refinement of the photoelastic technique used in this work), acoustic, strain gages, crack opening displacement and others.

Early standardization of specimen sizes and shapes for composite fatigue testing would be of value in insuring reproducibility of tests and thus of results. Such standardization, of course, can only come about after meaningful testing of different sizes and shapes has been conducted. The need for additional testing programs is thus re-emphasized. The absence of a standard specimen caused a relatively long delay in data-gathering for this work.

The effects of various parameters which were not investigated in this study provide fertile ground for follow-on work. Specifically, since most GRP materials are quite rate-sensitive, the effect of varying the testing frequency should be investigated within the limits where results are not influenced by specimen heat-up.

Because a significant effect on fatigue properties was noted after a salt water presoak period of only ten days (a negligible length of time in the life of a ship) the effect of longer presoak periods should be pursued in some detail. It is recommended that periods of 30 days and longer be used in future studies. In this regard, it is further recommended that a standard, synthetic sea water solution be used instead of the 3% sodium chloride solution to account for the possible effect of any trace elements. A standard mixture that would probably be acceptable is Synthetic Sea Salt available from Dayno Sales Company of Lynn, Massachusetts.

ACKNOWLEDGEMENTS

The general research program on the fracture behavior of fibrous reinforced composites, from which this report derives, receives support from The Dow Chemical Company, the Air Force Materials Laboratory (USAF Contract F33615-72-C-1686), the NOAA Office of Sea Grant, Grant No. NG-43-72, and the M.I.T. Center for Materials Science and Engineering (NSF Contract GH-33653). This support is gratefully acknowledged by the authors.

REFERENCES

1. "The GRP Minehunter", NAVAL RECORD, Oct., 1972.

2. F.J. McGarry and J.F. Mandell, "Fracture Toughness Studies of Fiber Reinforced Plastic Laminates", MIT, Dept. of Civil Engineering Report R72-5 (1972).

3. K. Masubuchi, Materials for Ocean Engineering, MIT Press, (1970).

4. J.F. Mandell and U. Meier, "Fatigue Crack Propagation in $0^{o}/90^{o}$ E-Glass/Epoxy Composites", to be published (1973).

5. R. Kashihara, Personal Communication, MIT, Dept. of Civil Engineering, Jan. 15, 1973.

6. J.F. Mandell and F.J. McGarry, "The Origins of Fracture Toughness in Fiber Reinforced Plastics: Model and Crossplied Laminate Studies", MIT, Dept. of Civil Engineering Report R72-11 (1972).

7. G.R. Irwin and J.A. Kies, WELDING JOURNAL, 1952, vol. 31, 95s.

8. J.E. Srawley and B. Gross, "Stress Intensity Factors for Crackline-Loaded Edge-Crack Specimens", NASA Technical Note D-3820 (1967).

9. B. Gross and J.E. Srawley, "Stress Intensity Factors by Boundary Collocation for Single-Edge-Notch Specimens Subject to Splitting Forces", NASA Technical Note D-3295 (1966).

10. D.L. Bowie,"Rectangular Tensile Sheet with Symmetric Edge Cracks", Paper 64-APM-3, ASME, (1964).

11. L.J. Broutman and R.H. Krock, Modern Composite Materials, Addison-Wesley, Reading, Mass., (1967), p. 404.

12. N. Fried and W.R. Graner, "Durability of Reinforced Plastic Structural Materials in Marine Service", MARINE TECHNOLOGY, July, 1966.

APPENDIX A.

FIGURES

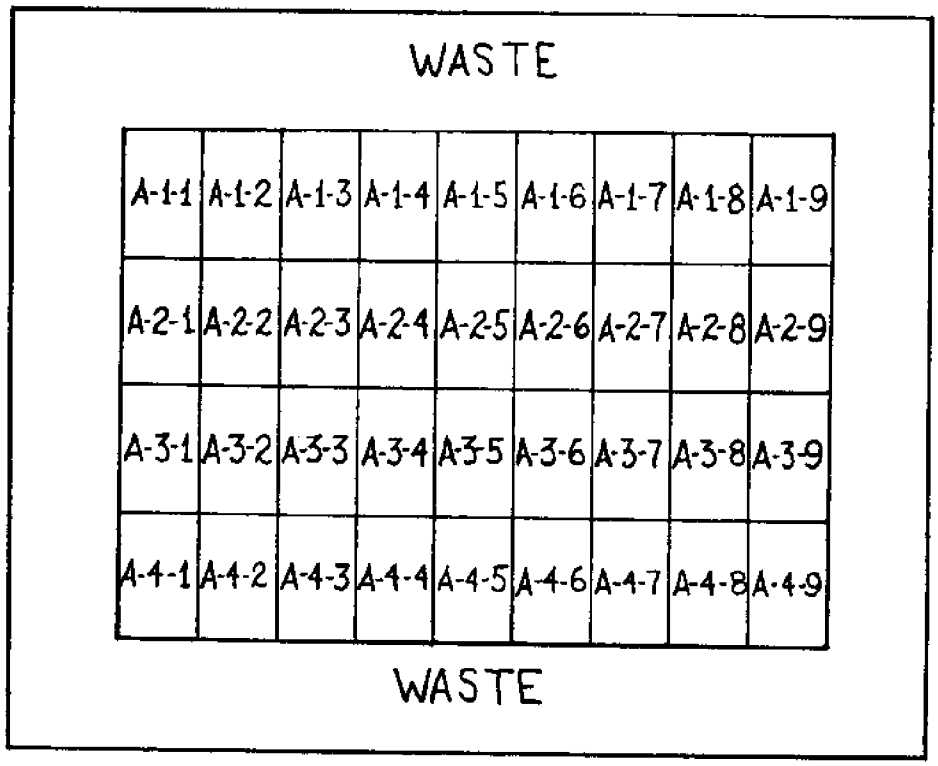

FIGURE 1a. SPECIMEN NUMBERING - Plate A
(36 index card specimens)

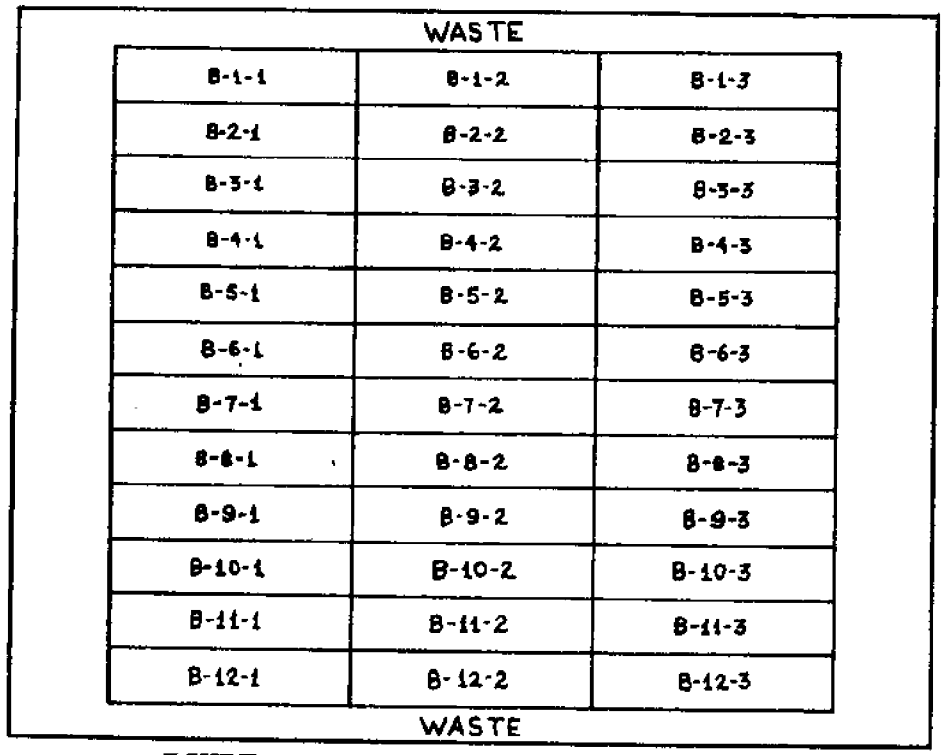

FIGURE 1b. SPECIMEN NUMBERING - Plate B
(36 dogbone specimens)

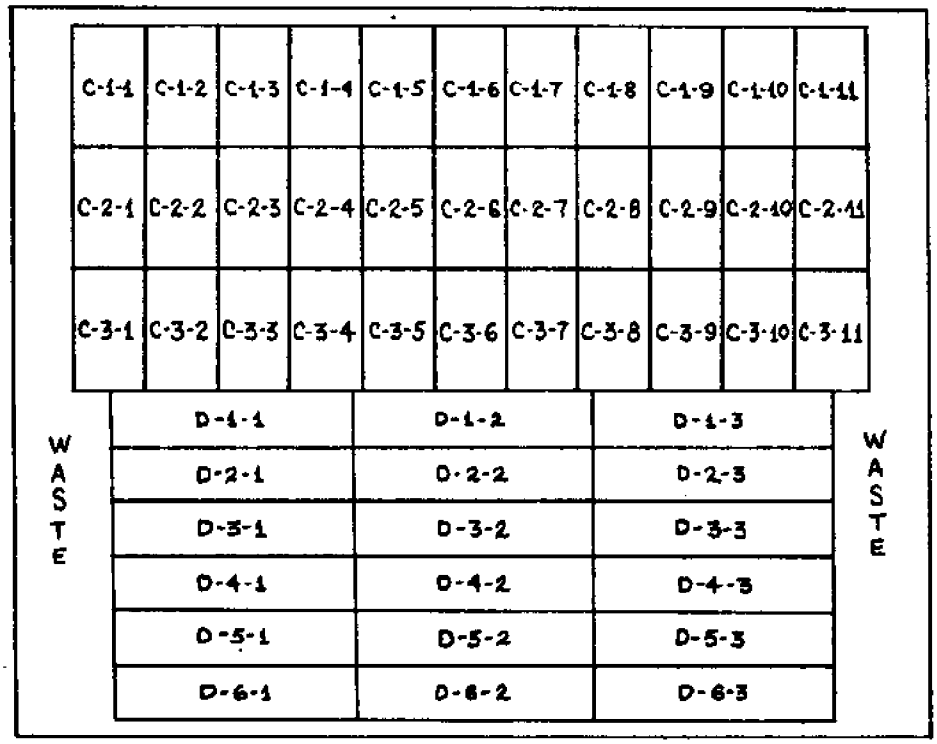

FIGURE 1c. SPECIMEN NUMBERING - Plate C/D
(33 index card and 18 dogbone specimens)

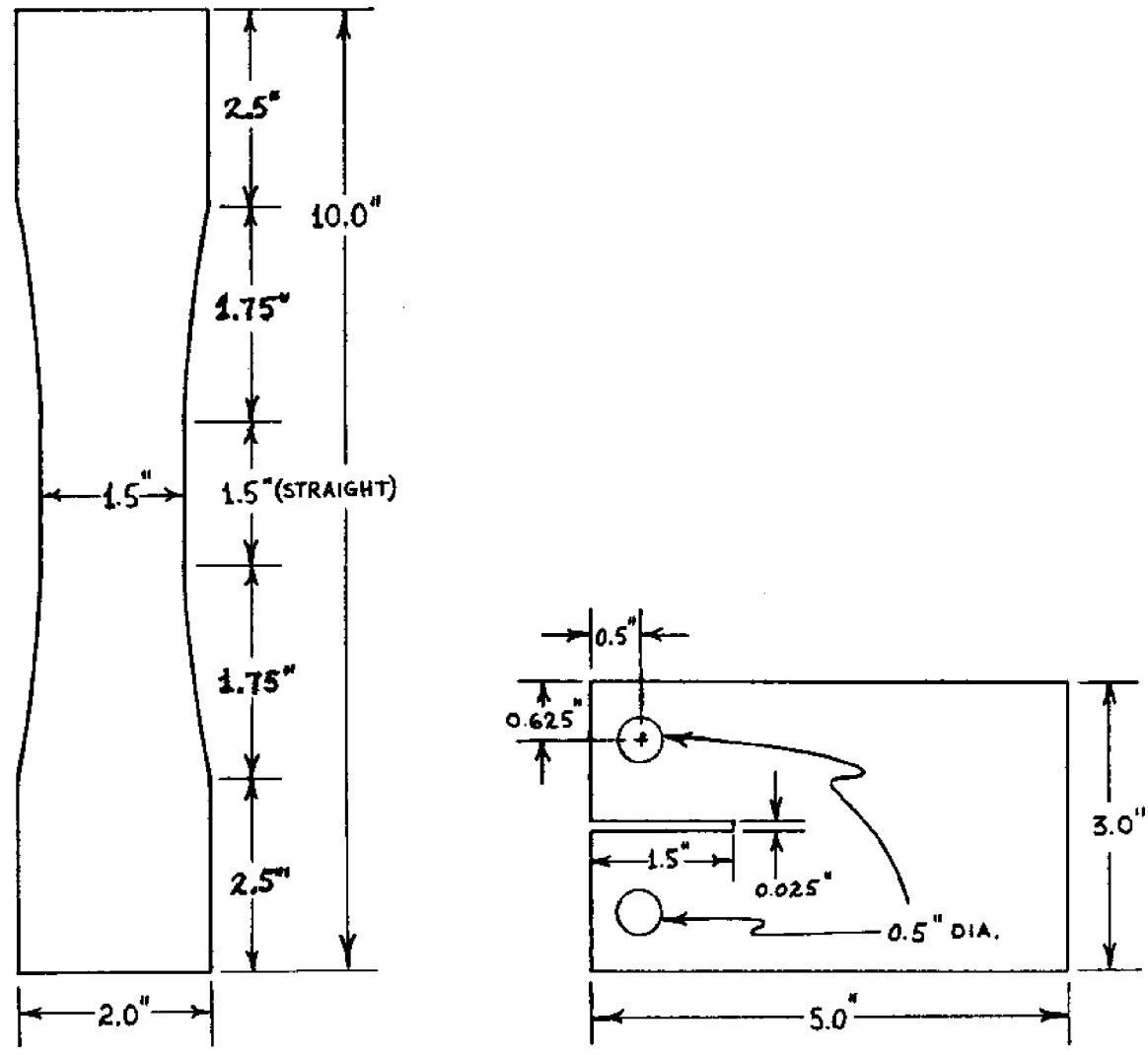

UNNOTCHED
(Dogbone)

NOTCHED
(Index Card)

FIGURE 2. FATIGUE SPECIMEN GEOMETRY

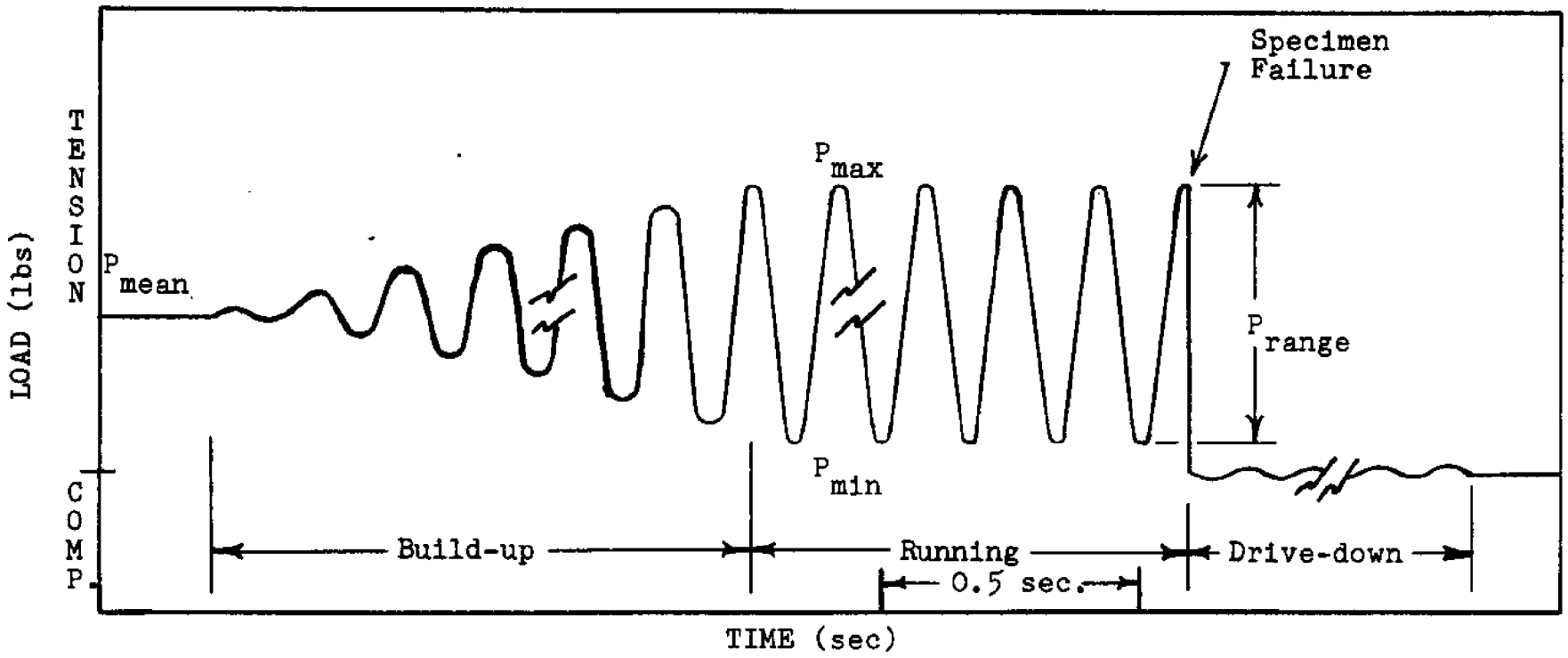

FIGURE 3. FATIGUE LOAD CYCLE CHARACTERISTICS

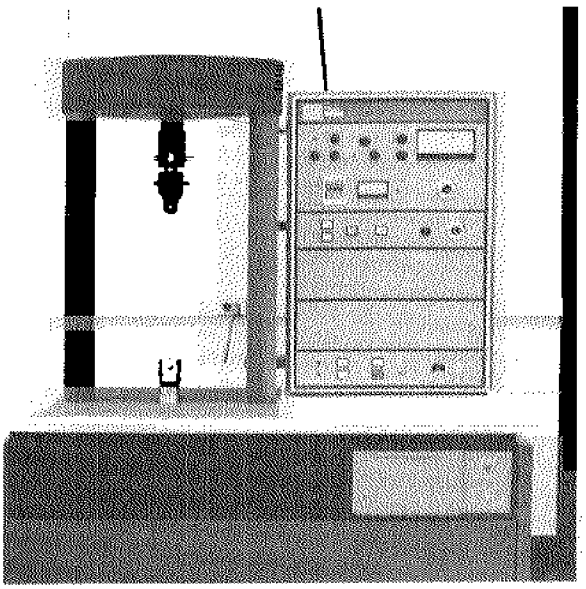

FIGURE 4a.

INSTRON MODEL 1211 DYNAMIC CYCLER

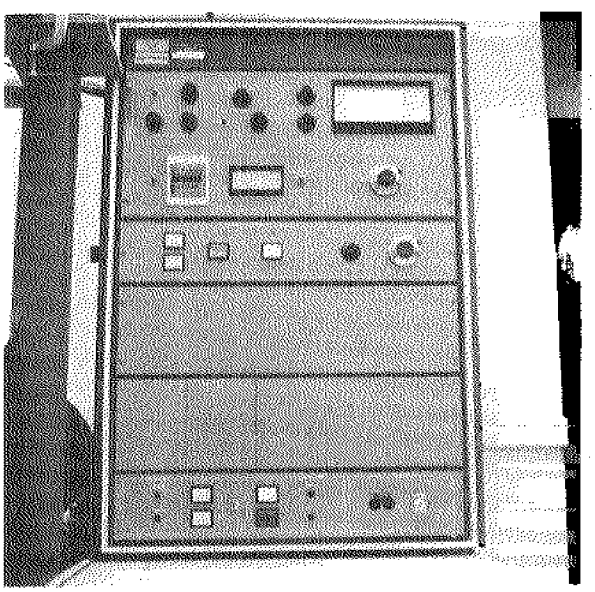

FIGURE 4b.

CONTROL PANEL OF MODEL 1211

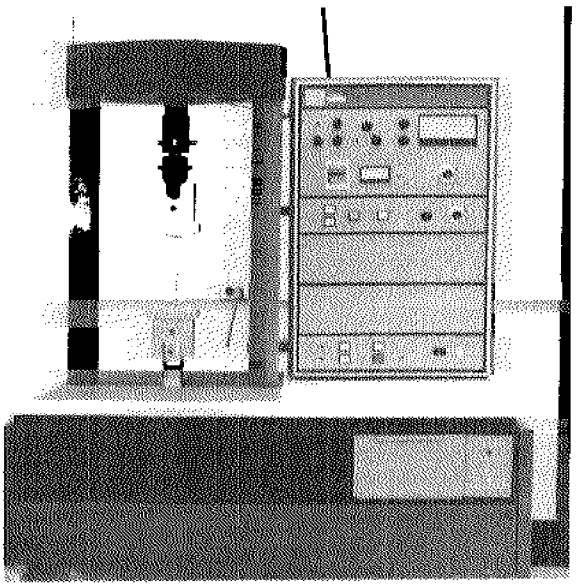

FIGURE 4c.

MODEL 1211 WITH UNNOTCHED (DOGBONE)
SPECIMEN INSTALLED

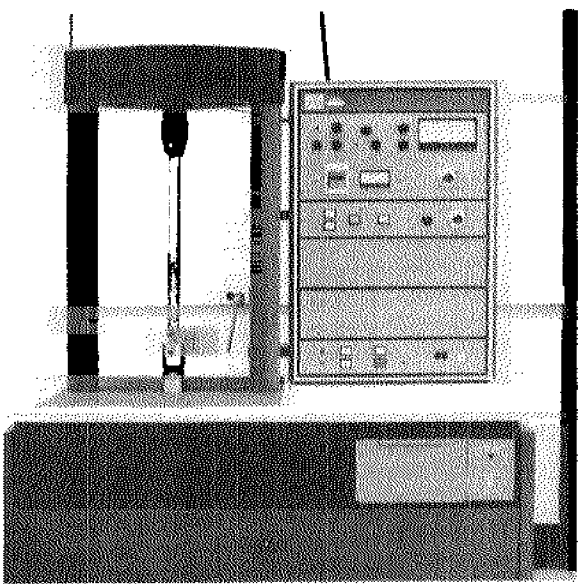

FIGURE 4d.

MODEL1211 WITH NOTCHED (INDEX CARD)
SPECIMEN INSTALLED

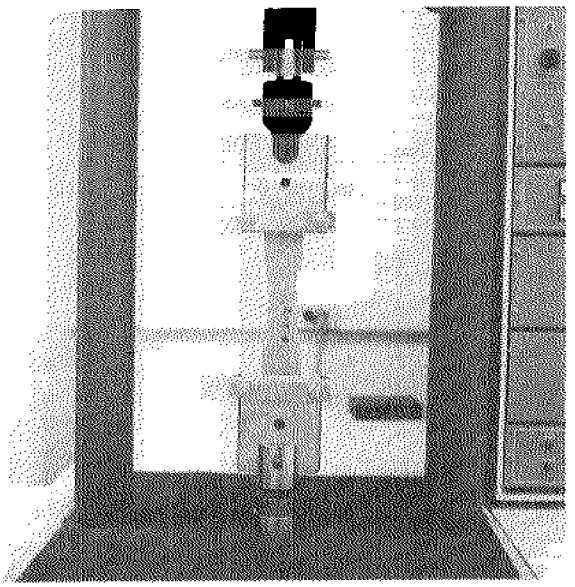

FIGURE 5a.

SPECIMEN GRIPPING ASSEMBLY
(UNNOTCHED SPECIMENS)

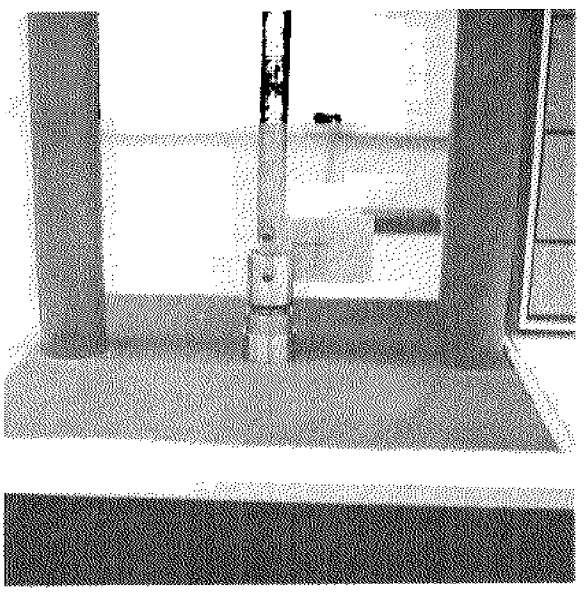

FIGURE 5b.

SPECIMEN GRIPPING ASSEMBLY
(NOTCHED SPECIMENS)

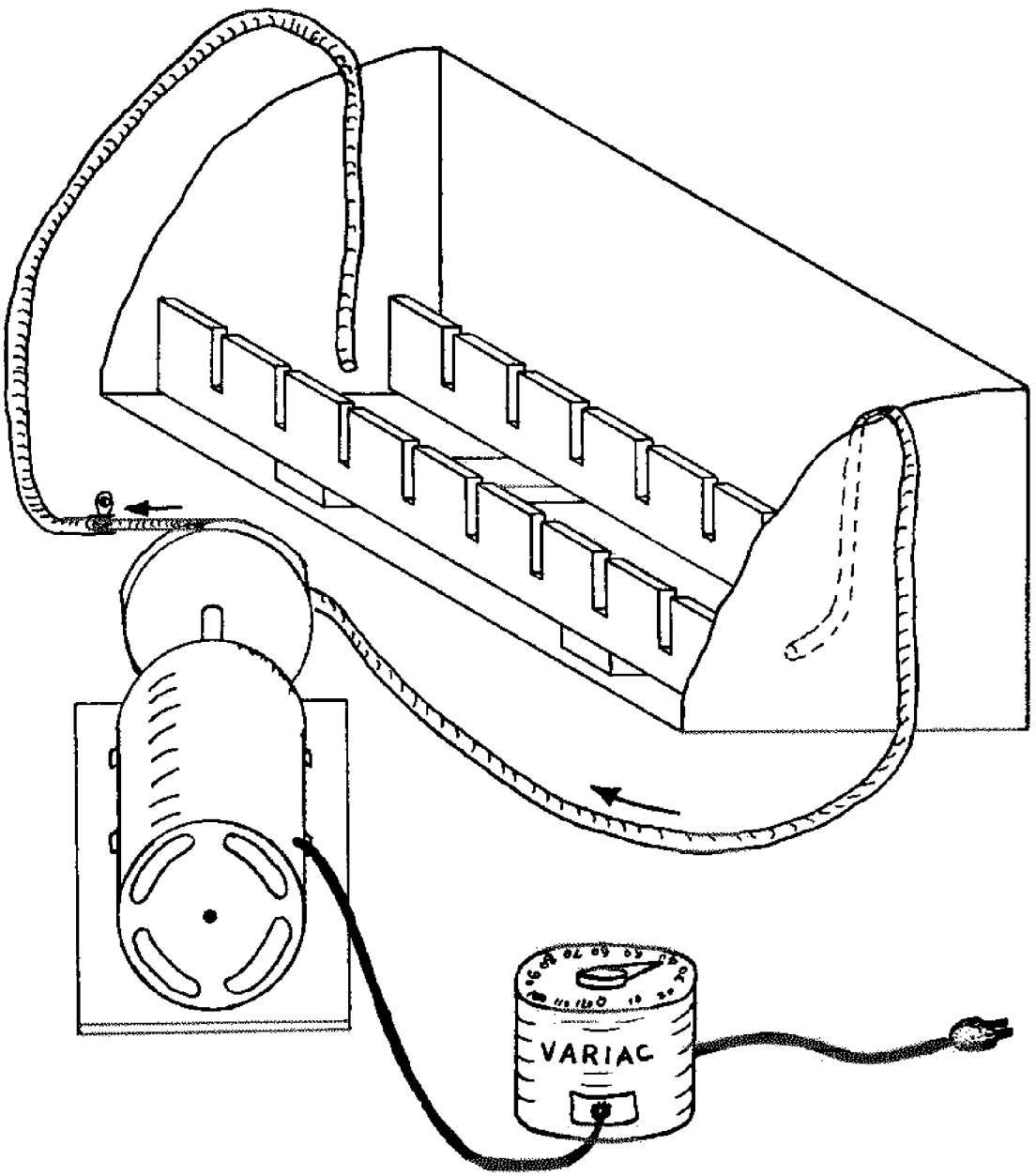

FIGURE 6. CIRCULATING SALT WATER PRESOAK BATH

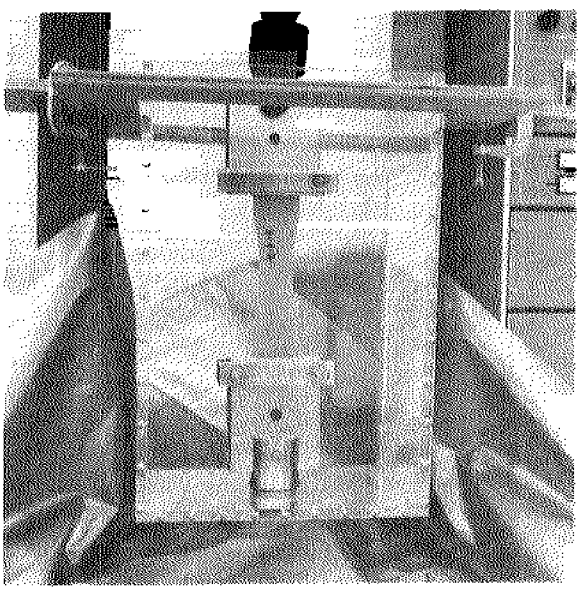

FIGURE 7.

SALT WATER CONTAINMENT SYSTEM
(SHOWN INSTALLED ON MODEL 1211)

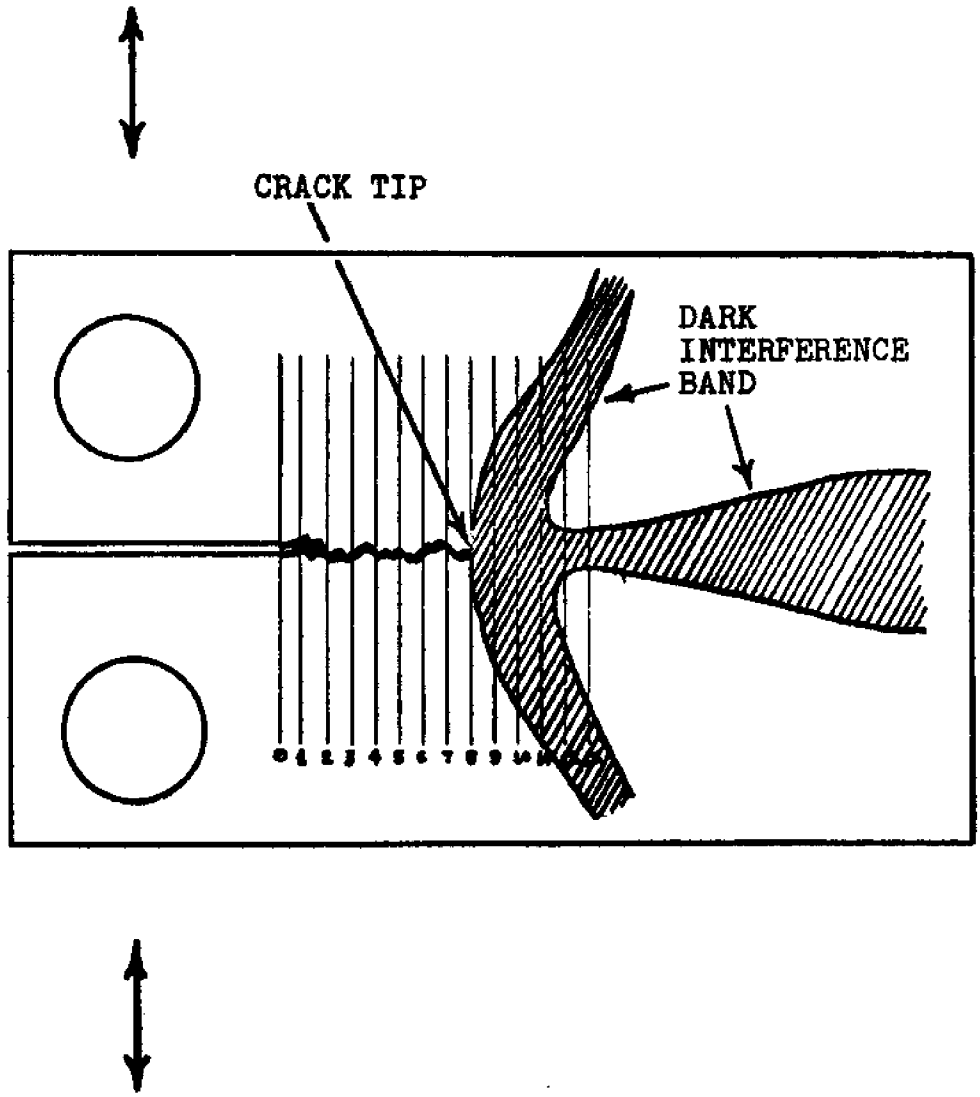

FIGURE 8.

LOCATION OF FATIGUE CRACK TIP
(SPECIMEN VIEWED THROUGH CROSS-POLARIZED LIGHT)

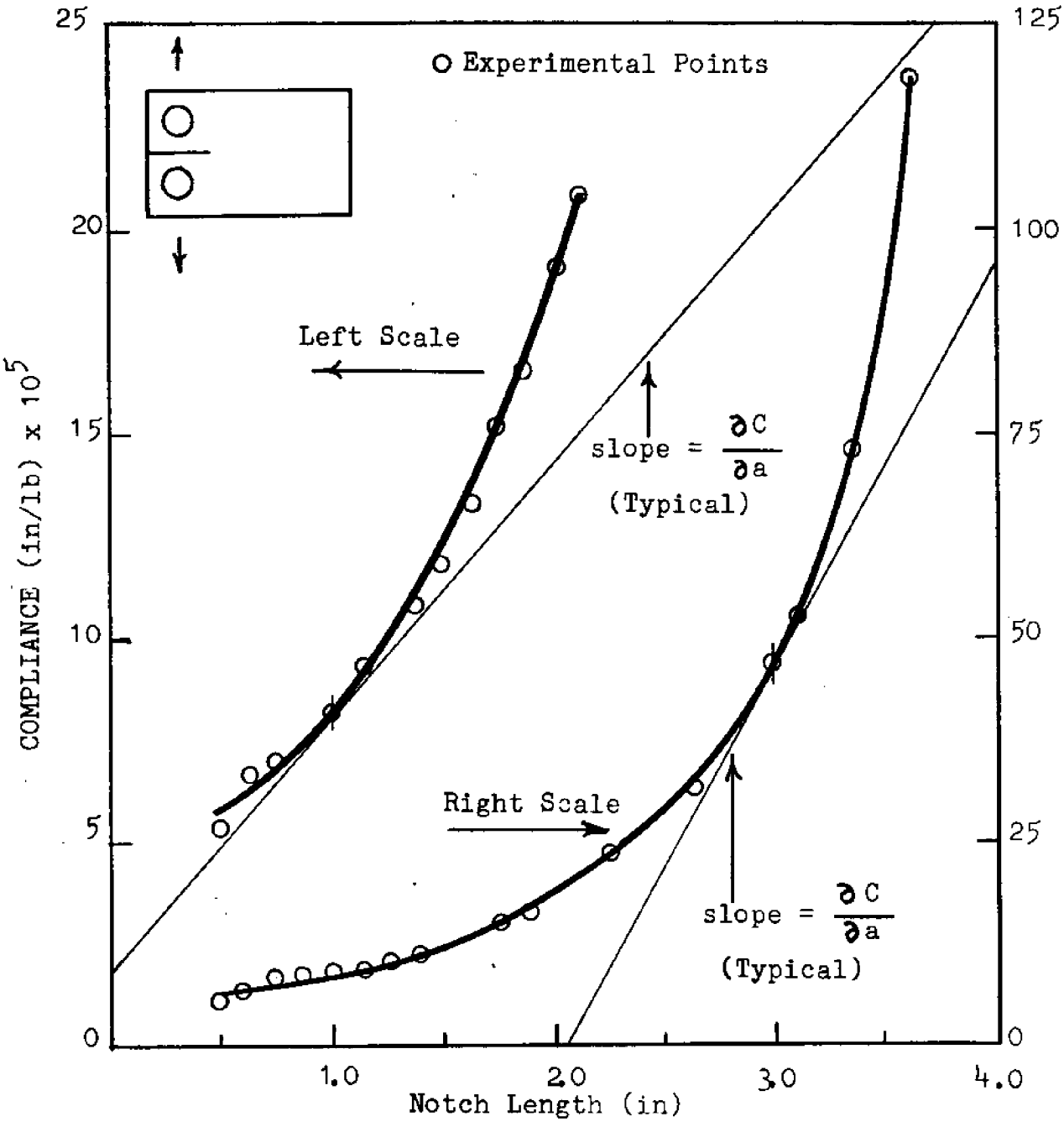

FIGURE 9.

COMPLIANCE VS NOTCH LENGTH FOR IRWIN-KIES K-CALIBRATION

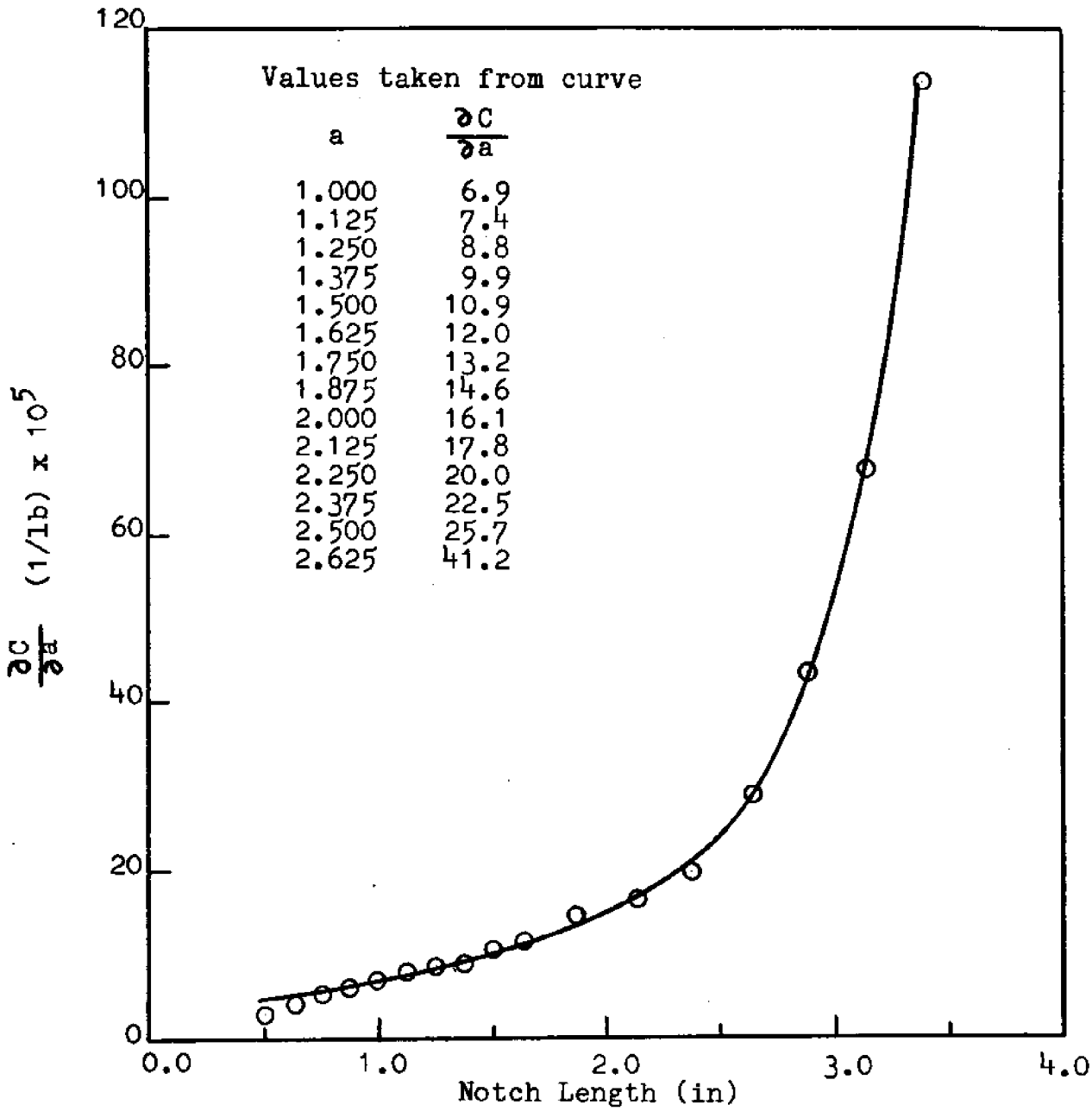

FIGURE 10.

$\frac{\partial C}{\partial a}$ VS NOTCH LENGTH FOR K-CALIBRATION

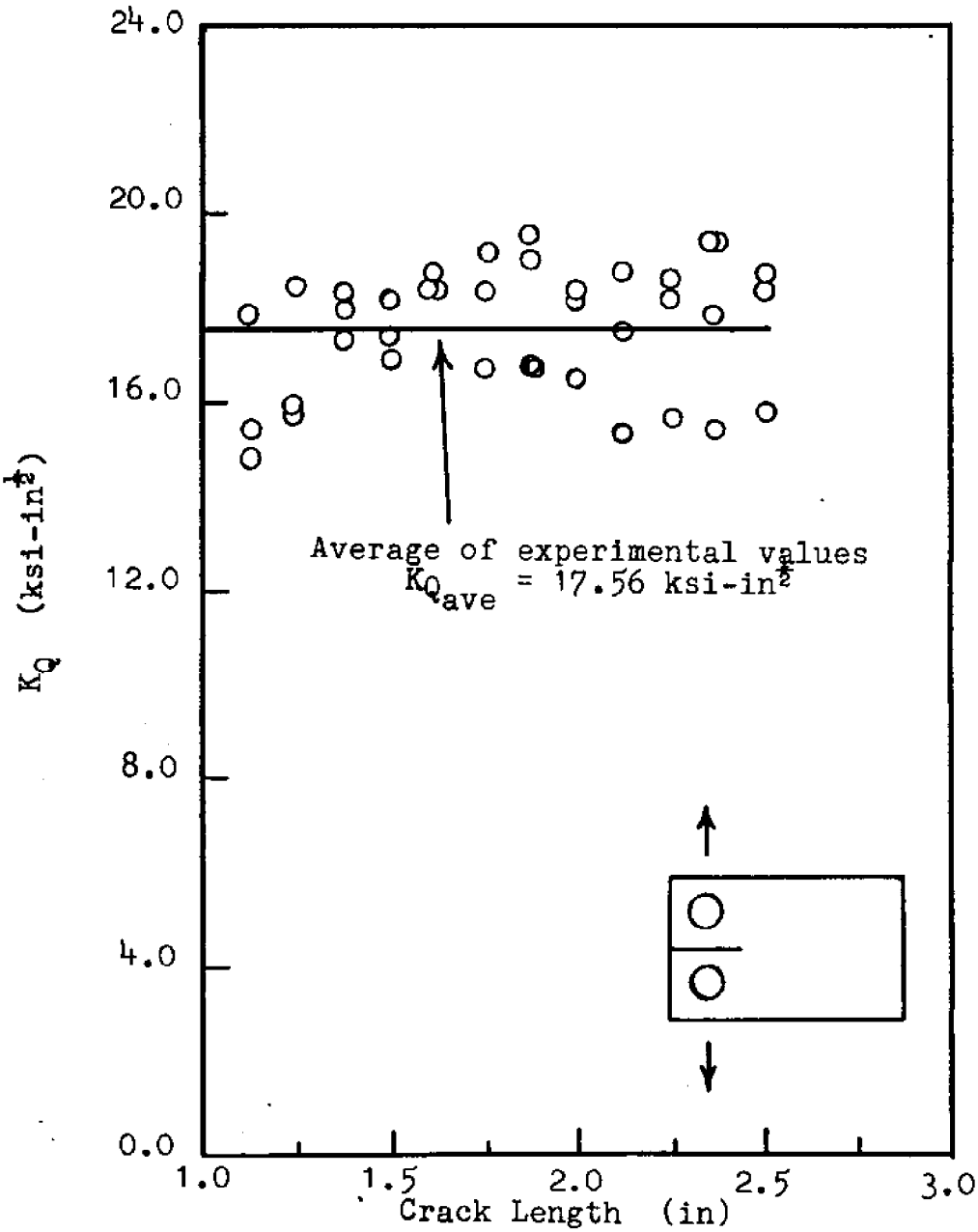

FIGURE 11.

K_Q VS CRACK LENGTH

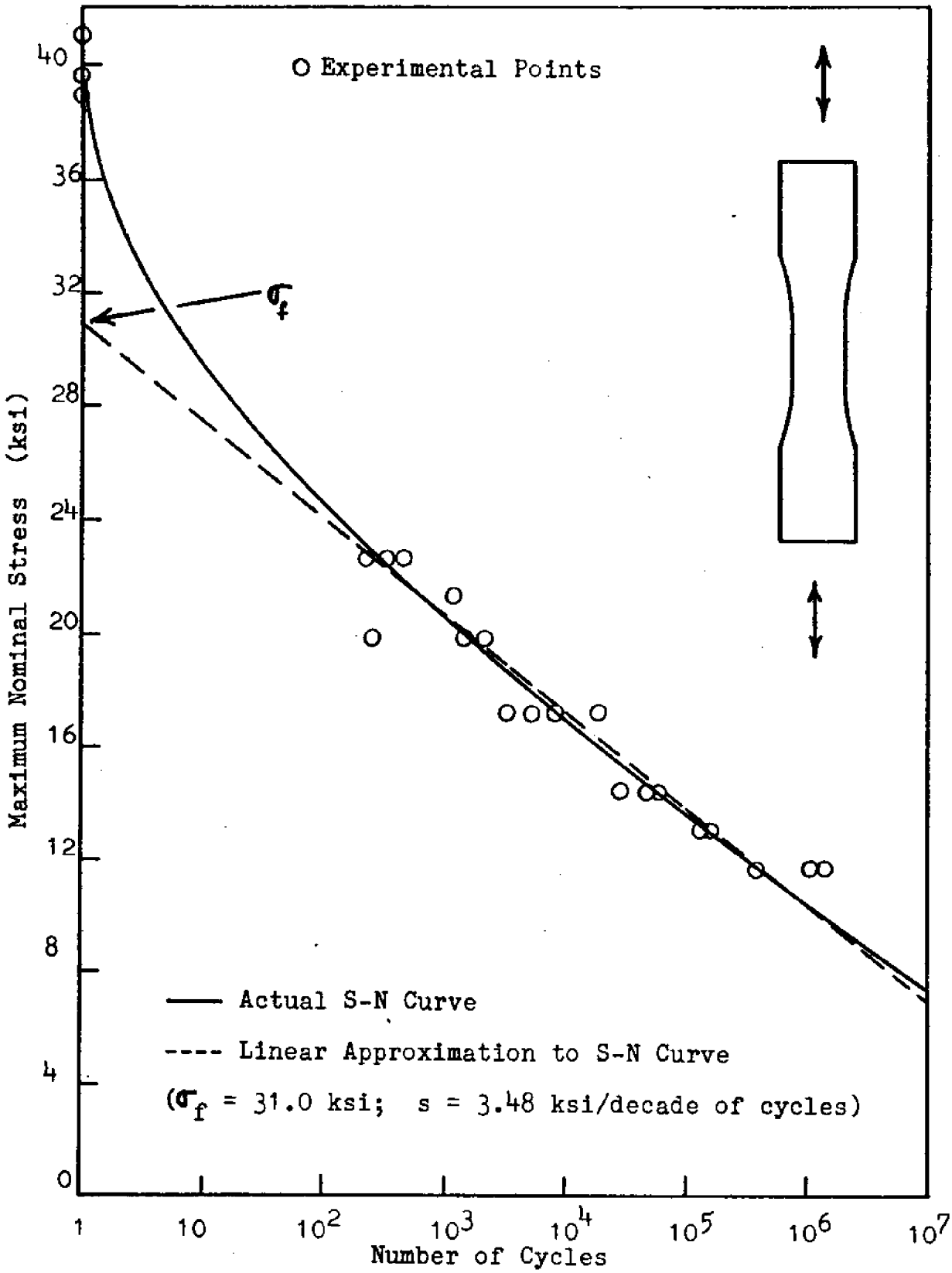

FIGURE 12. S-N CURVE (DRY ENVIRONMENT)

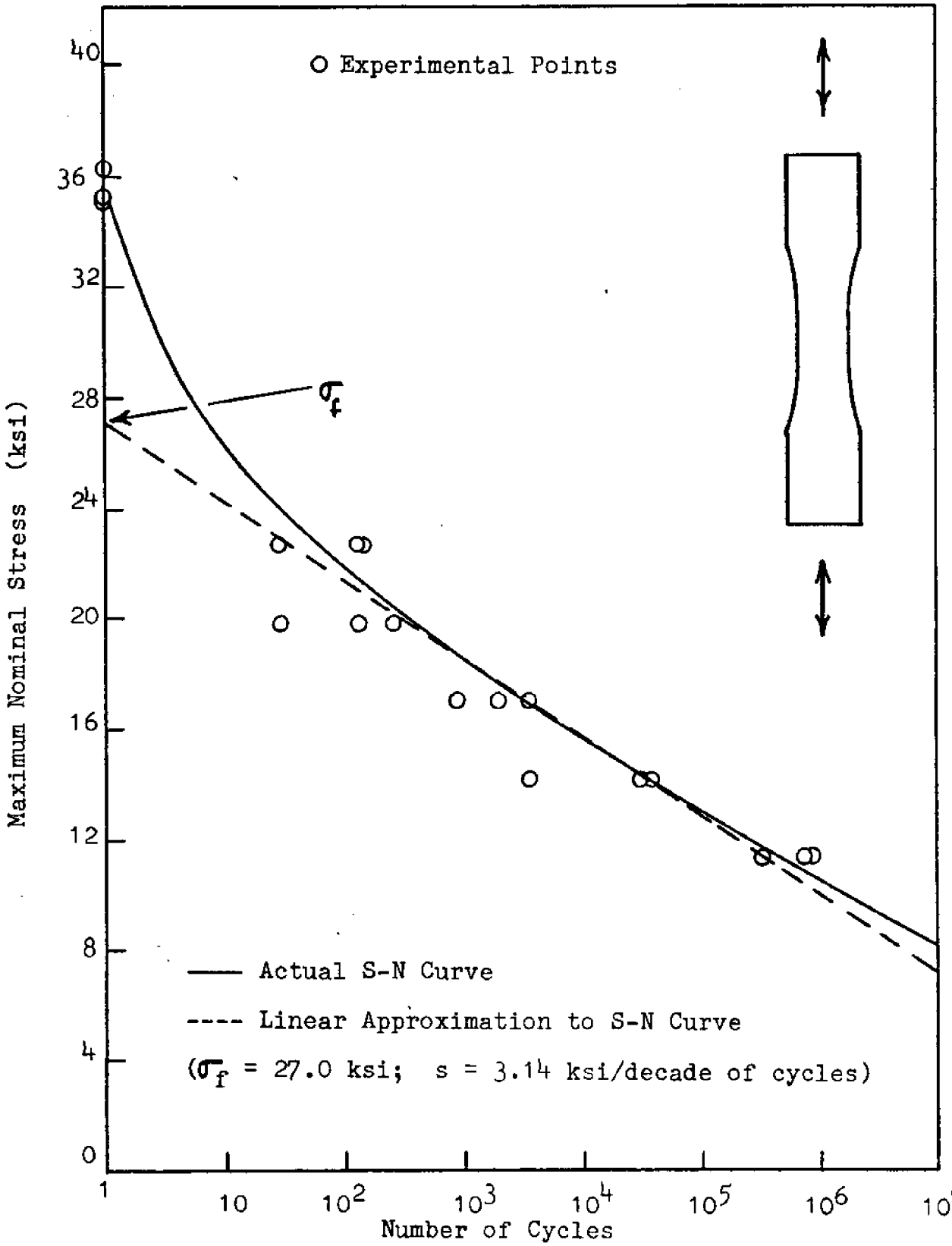

FIGURE 13. S-N CURVE (SALT WATER ENVIRONMENT)

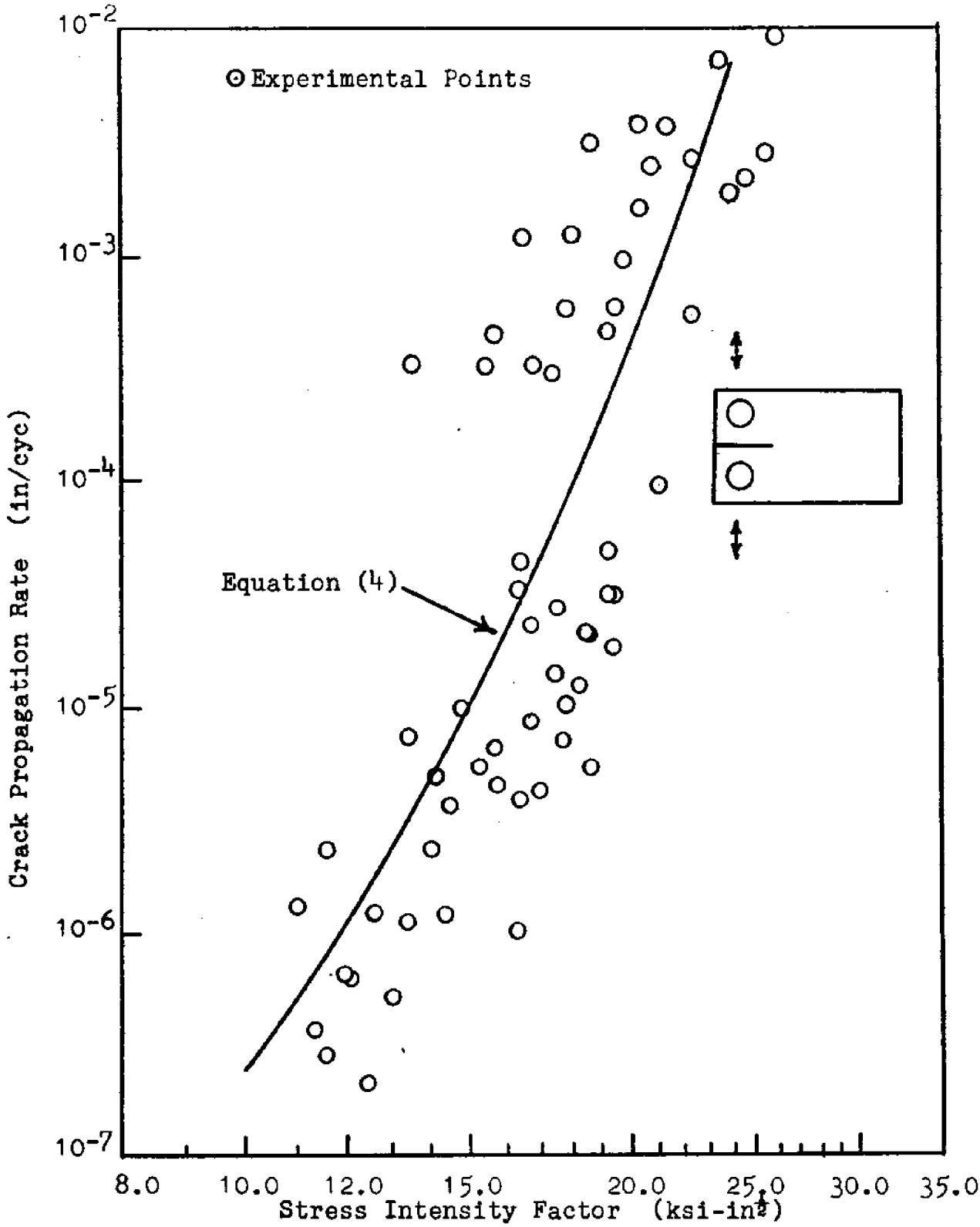

FIGURE 14. FATIGUE CRACK PROPAGATION RATE VS STRESS INTENSITY FACTOR (DRY ENVIRONMENT)

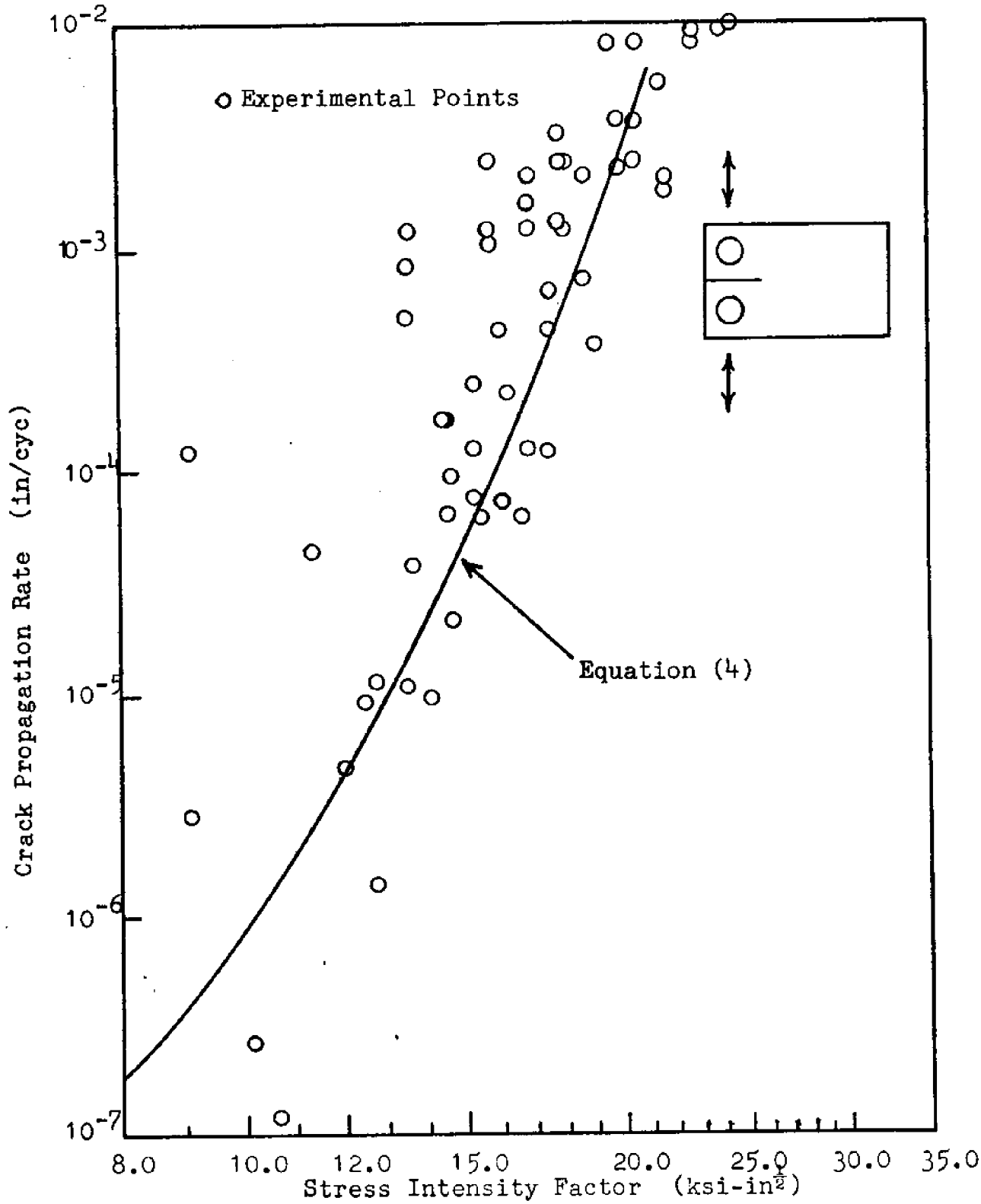

FIGURE 15. FATIGUE CRACK PROPAGATION RATE VS STRESS INTENSITY FACTOR (SALT WATER ENVIRONMENT)

APPENDIX B.

TABLES

TABLE 1a.

FATIGUE LOADING CONDITIONS - UNNOTCHED SPECIMENS

(UTS_{est} = 9200 lbs. Load cycles are designated by;

$$\frac{P_{max}}{UTS_{est}} \times 100\%.)$$

Load Cycle	40%	50%	60%	70%	80%
P_{max}	3680	4600	5520	6440	7360
P_{min}	400	400	400	400	400
P_{range}	3280	4200	5120	6040	6960
P_{mean}	2040	2500	2960	3420	3880

TABLE 1b.

FATIGUE LOADING CONDITIONS - NOTCHED SPECIMENS

(UTS_{est} = 1200 lbs. Load cycles are designated by;

$$\frac{P_{max}}{UTS_{est}} \times 100\%.)$$

Load Cycle	40%	50%	60%	70%	80%
P_{max}	480	600	720	840	960
P_{min}	80	80	80	80	80
P_{range}	400	520	640	760	880
P_{mean}	280	340	400	460	520

TABLE 2a.

ULTIMATE TENSILE STRENGTH DATA - UNNOTCHED SPECIMENS

(Strain rate = 60 in/min)

Specimen	Environment	Nominal Stress at Failure (psi)
B-2-2	Dry	41,148
B-9-1	Dry	38,975
B-3-2	Dry	39,654
B-2-1	Salt Water	36,123
B-7-1	Salt Water	35,105
D-5-1	Salt Water	35,309

$$\frac{\text{Average S.W. UTS}}{\text{Average Dry UTS}} = 0.89$$

TABLE 2b.

ULTIMATE SUSTAINED LOAD - NOTCHED SPECIMENS

(Strain rate = 30 in/min. Notch length - 1.0 inch from line of load application.)

Specimen	Environment	Load at Failure (lbs)	K_Q (ksi-in$^{\frac{1}{2}}$) from eq. (6)
C-1-8	Dry	1606	28.7
C-2-2	Dry	1439	25.7
C-2-5	Dry	1518	27.1
C-3-5	Dry	1661	29.6
C-1-5	Salt Water	1408	25.1
C-2-6	Salt Water	1408	25.1
C-2-11	Salt Water	1338	23.9

TABLE 3.

IRWIN-KIES K-CALIBRATION DATA

Notch Length a (in)	Average Compliance C_{ave} (in/lb) x10^5	$\frac{\partial C}{\partial a}$ (1/lb) x10^5
0.500	5.29	3.66
0.625	6.66	4.54
0.750	6.95	5.24
0.875	7.29	5.77
1.000	8.22	6.67
1.125	9.28	7.39
1.250	10.1	8.50
1.375	10.8	9.60
1.500	11.8	10.7
1.625	13.2	12.0
1.875	16.4	15.0
2.125	20.8	17.1
2.375	25.4	20.1
2.625	32.0	29.5
2.875	40.6	43.6
3.125	54.1	67.4
3.375	74.4	114

Specimens A-1-4, A-1-9 and A-3-9 were used for this K-calibration.

TABLE 4.

BOUNDARY COLLOCATION K-CALIBRATION DATA

$$K = P(8.72a + 9.13)$$

P_{max} (lbs) (Load Cycle)	Crack Length (in)	K (ksi-in$^{\frac{1}{2}}$)
480 (40%)	1.125	9.09
	1.250	9.62
	1.375	10.1
	1.500	10.7
	1.625	11.2
	1.750	11.7
	1.875	12.2
	2.000	12.8
	2.125	13.3
	2.250	13.8
	2.375	14.3
	2.500	14.9
600 (50%)	1.125	11.4
	1.250	12.0
	1.375	12.7
	1.500	13.3
	1.625	14.0
	1.750	14.6
	1.875	15.3
	2.000	15.9
	2.125	16.6
	2.250	17.2
	2.375	17.9
	2.500	18.6
720 (60%)	1.125	13.6
	1.250	14.4
	1.375	15.2
	1.500	16.0
	1.625	16.8
	1.750	17.6
	1.875	18.3
	2.000	19.1
	2.125	19.9
	2.250	20.7
	2.375	21.5
	2.500	22.3

TABLE 4,
(cont'd)

P_{max} (lbs) (Load Cycle)	Crack Length (in)	K ($ksi\text{-}in^{\frac{1}{2}}$)
840 (70%)	1.125	15.9
	1.250	16.8
	1.375	17.7
	1.500	18.6
	1.625	19.6
	1.750	20.5
	1.875	21.4
	2.000	22.3
	2.125	23.3
	2.250	24.1
	2.375	25.1
	2.500	26.0
960 (80%)	1.125	18.2
	1.250	19.2
	1.375	20.3
	1.500	21.3
	1.625	22.4
	1.750	23.4
	1.875	24.5
	2.000	25.5
	2.125	26.5
	2.250	27.6
	2.375	28.6
	2.500	29.7

TABLE 5

K_Q-CALIBRATION DATA

Specimen	Crack Length a (in)	Load P (lb)	$\frac{\partial C}{\partial a} \times 10^5$ (1/lb)	G (lb/in)	K_Q (ksi-in$^{\frac{1}{2}}$)
C-1-6	1.125	950	7.8	163	17.8
	1.250	930	8.8	176	18.5
	1.375	850	9.9	166	18.0
	1.500	810	10.9	154	17.3
	1.625	790	12.0	173	18.4
	1.750	780	13.2	186	19.1
	1.875	740	14.6	185	19.0
	2.000	680	16.1	172	18.3
	2.125	620	17.8	158	17.5
	2.250	620	20.0	178	18.6
	2.375	610	22.5	194	19.4
	2.500	550	25.7	180	18.7
C-2-1	1.125	790	7.8	113	14.8
	1.250	790	8.8	127	15.7
	1.375	820	9.9	154	17.3
	1.500	760	10.9	146	16.9
	1.625	790	12.0	173	18.4
	1.750	680	13.2	141	16.6
	1.875	650	14.6	143	16.7
	2.000	610	16.1	139	16.5
	2.125	540	17.8	120	15.3
	2.250	520	20.0	125	15.6
	2.375	480	22.5	120	15.3
	2.500	460	25.7	126	15.7
C-2-8	1.125	820	7.8	121	15.4
	1.250	800	8.8	130	15.9
	1.375	870	9.9	173	18.4
	1.500	820	10.9	170	18.2
	1.625	800	12.0	178	18.6
	1.750	750	13.2	172	18.3
	1.875	760	14.6	195	19.5
	2.000	670	16.1	167	18.1
	2.125	660	17.8	179	18.7
	2.250	600	20.0	167	18.1
	2.375	600	22.5	188	19.3
	2.500	540	25.7	173	18.4

TABLE 6

FATIGUE FAILURE DATA - UNNOTCHED SPECIMENS

(DRY ENVIRONMENT)

Load Cycle	Maximum Nominal Stress (psi)	Specimen	Cycles to Failure
40%	11,358	B-11-1	1,069,000
		B-12-2	1,606,000
		D-5-3	395,000
45%	12,778	B-3-3	128,000
		B-9-3	147,000
50%	14,198	B-9-2	72,900
		D-2-2	27,400
		D-2-3	38,600
60%	17,037	B-4-1	17,400
		B-5-1	8,750
		B-7-3	2,970
		B-1-2	5,450
70%	19,877	B-6-2	2,100
		D-3-3	1,490
		D-6-3	280
75%	21,296	B-4-3	1,300
80%	22,716	B-1-3	300
		D-1-1	240
		D-4-2	460

TABLE 7

FATIGUE FAILURE DATA - UNNOTCHED SPECIMENS

(SALT WATER ENVIRONMENT AFTER 10-DAY SALT WATER PRESOAK)

Load Cycle	Maximum Nominal Stress (psi)	Specimen	Cycles to Failure
40%	11,358	B-1-1	576,000
		B-4-2	589,000
		B-7-2	320,000
50%	14,198	B-2-3	30,200
		B-5-2	38,700
		D-6-1	3,450
60%	17,037	B-12-1	910
		D-3-2	3,600
		D-4-1	2,070
70%	19,877	B-3-1	140
		D-1-3	270
		D-6-2	30
80%	22,716	B-8-2	140
		B-11-2	30
		B-12-3	140

TABLE 8.

THEORETICAL FATIGUE FAILURE DATA - NOTCHED SPECIMENS

(DRY ENVIRONMENT)

(σ_f = 31.0 ksi; s = 3.48 ksi per decade of cycles; K_Q = 27.8 ksi-in$^{\frac{1}{2}}$)

K (ksi-in$^{\frac{1}{2}}$)	$\exp\left[-2.3\frac{\sigma_f}{s}(1-\frac{K}{K_Q})\right]$ (cycles)	$\frac{da}{dN}$ (in/cyc)
10	2.0×10^{-6}	2.5×10^{-7}
11	4.4×10^{-6}	5.5×10^{-7}
12	8.3×10^{-6}	1.0×10^{-6}
13	1.8×10^{-5}	2.2×10^{-6}
14	3.6×10^{-5}	4.5×10^{-6}
15	8.0×10^{-5}	1.0×10^{-5}
16	1.8×10^{-4}	2.2×10^{-5}
17	3.4×10^{-4}	4.2×10^{-5}
18	7.7×10^{-3}	9.6×10^{-5}
19	1.4×10^{-3}	1.8×10^{-4}
20	3.2×10^{-3}	4.0×10^{-4}
21	7.2×10^{-3}	9.0×10^{-4}
22	1.4×10^{-2}	1.7×10^{-3}
23	3.1×10^{-2}	3.9×10^{-3}
24	5.6×10^{-1}	7.1×10^{-3}
25	1.3×10^{-1}	1.6×10^{-2}

TABLE 9.

EXPERIMENTAL FATIGUE FAILURE DATA - NOTCHED SPECIMENS

(DRY ENVIRONMENT)

Specimen (Load Cycle)	Crack Length (in)	Crack Growth Rate (in/cyc)	K (ksi-in$^{\frac{1}{2}}$)
C-3-1 (50%)	1.250	5.62×10^{-7}	12.0
	1.275	5.43×10^{-7}	12.1
	1.500	1.10×10^{-6}	13.3
	1.687	1.20×10^{-6}	14.3
	1.937	4.38×10^{-6}	15.8
	2.375	4.86×10^{-5}	19.1
C-2-7 (50%)	1.125	3.57×10^{-7}	11.3
	1.187	2.31×10^{-6}	11.6
	1.312	2.11×10^{-7}	12.4
	1.375	1.18×10^{-6}	12.7
A-2-2 (50%)	1.062	1.30×10^{-6}	11.0
	1.187	2.85×10^{-7}	11.6
	1.437	5.04×10^{-7}	13.0
	1.625	2.34×10^{-6}	14.0
	2.000	1.01×10^{-6}	16.2
	2.312	5.21×10^{-6}	18.6
A-1-7 (60%)	1.094	7.44×10^{-6}	13.3
	1.219	4.88×10^{-6}	14.1
	1.312	9.97×10^{-6}	14.8
	1.469	6.68×10^{-6}	15.7
	1.656	4.08×10^{-5}	17.0
	1.750	2.75×10^{-4}	17.5
C-1-2 (60%)	1.125	3.21×10^{-6}	13.5
	1.250	3.61×10^{-6}	14.4
	1.375	5.21×10^{-6}	15.2
	1.562	3.83×10^{-5}	16.3
	1.750	1.44×10^{-5}	17.5
	1.875	2.08×10^{-3}	18.5
A-2-3 (70%)	1.187	1.17×10^{-4}	16.3
	1.250	3.12×10^{-4}	16.8
	1.312	2.98×10^{-4}	17.3
	1.375	5.68×10^{-4}	17.8
	1.562	4.46×10^{-4}	19.1
	1.625	5.68×10^{-3}	19.5
	1.750	1.56×10^{-3}	20.5
	1.937	2.68×10^{-3}	22.2
	2.500	1.88×10^{-2}	28.6

TABLE 9.
(cont'd)

Specimen (Load Cycle)	Crack Length (in)	Crack Growth Rate (in/cyc)	K (ksi-in$^{\frac{1}{2}}$)
C-1-9 (70%)	1.125	4.17×10^{-4}	15.7
	1.187	4.16×10^{-5}	16.3
	1.250	2.31×10^{-5}	16.8
	1.375	7.14×10^{-6}	17.8
	1.437	1.25×10^{-5}	18.2
	1.500	2.08×10^{-5}	18.6
	1.625	1.78×10^{-5}	19.5
	1.812	9.37×10^{-5}	21.0
	2.250	2.92×10^{-4}	25.3
C-2-3 (70%)	1.062	3.12×10^{-5}	15.4
	1.187	3.28×10^{-5}	16.3
	1.250	7.81×10^{-6}	16.8
	1.375	1.04×10^{-5}	17.8
	1.562	3.12×10^{-5}	19.1
	1.625	3.12×10^{-5}	19.5
	1.937	5.21×10^{-4}	22.2
	2.125	1.88×10^{-3}	23.8
A-2-6 (80%)	1.875	2.19×10^{-3}	24.6
A-4-4 (80%)	1.250	4.17×10^{-3}	19.2
	1.500	1.25×10^{-2}	21.3
	1.875	1.25×10^{-2}	24.6
	2.625	1.88×10^{-2}	41.4
C-2-9 (80%)	1.125	1.25×10^{-3}	18.0
	1.312	9.38×10^{-4}	19.8
	1.437	2.50×10^{-3}	20.8
	1.500	3.75×10^{-3}	21.3
	2.000	9.38×10^{-3}	25.9
C-3-2 (80%)	1.187	3.12×10^{-3}	18.6
	1.375	3.75×10^{-3}	20.3
	1.750	7.50×10^{-3}	23.5
	2.375	1.04×10^{-2}	30.6

TABLE 10.

THEORETICAL FATIGUE FAILURE DATA - NOTCHED SPECIMENS

(SALT WATER ENVIRONMENT)

(σ_f = 27.0 ksi; $_1s$ = 3.14 ksi pre decade of cycles; $K_Q{}^f$ = 24.8 ksi-in$^{\frac{1}{2}}$)

K (ksi-in$^{\frac{1}{2}}$)	$\exp\left[-2.3\frac{\sigma_f}{s}(1-\frac{K}{K_Q})\right]$ (cycles)	$\frac{da}{dN}$ (in/cyc)
8	1.5×10^{-6}	1.9×10^{-7}
9	3.1×10^{-6}	3.8×10^{-7}
10	6.8×10^{-6}	8.4×10^{-7}
11	1.5×10^{-5}	1.8×10^{-6}
12	3.4×10^{-5}	4.2×10^{-6}
13	1.1×10^{-4}	1.4×10^{-5}
14	1.7×10^{-4}	2.1×10^{-5}
15	3.7×10^{-4}	4.6×10^{-5}
16	9.9×10^{-4}	1.2×10^{-4}
17	2.2×10^{-3}	2.7×10^{-4}
18	4.8×10^{-3}	6.0×10^{-4}
19	1.0×10^{-2}	1.3×10^{-3}
20	2.3×10^{-2}	2.9×10^{-3}
21	5.1×10^{-2}	6.4×10^{-3}
22	1.1×10^{-1}	1.4×10^{-2}

TABLE 11.

EXPERIMENTAL FATIGUE FAILURE DATA - NOTCHED SPECIMENS

(SALT WATER ENVIRONMENT)

Specimen (Load Cycle)	Crack Length (in)	Crack Growth Rate (in/cyc)	K ($ksi\text{-}in^{\frac{1}{2}}$)
C-3-6 (40%)	1.125	2.78×10^{-6}	9.01
	1.375	2.60×10^{-7}	10.1
	1.500	1.21×10^{-7}	10.6
C-1-1 (50%)	1.125	1.25×10^{-4}	9.01
	1.312	9.10×10^{-6}	12.4
	1.375	1.13×10^{-5}	12.7
	1.562	3.75×10^{-5}	13.6
	1.750	9.37×10^{-5}	14.6
	2.000	2.27×10^{-4}	16.2
C-3-7 (50%)	1.125	4.16×10^{-5}	11.3
	1.250	4.60×10^{-6}	12.0
	1.375	1.40×10^{-6}	12.7
	1.500	1.04×10^{-5}	13.3
	1.625	9.60×10^{-6}	14.0
	1.750	2.08×10^{-5}	14.6
	1.875	6.25×10^{-5}	15.4
	2.062	6.25×10^{-5}	16.6
	2.187	1.25×10^{-4}	17.5
C-1-4 (60%)	1.125	1.25×10^{-3}	13.5
	1.250	6.57×10^{-4}	14.4
	1.375	2.50×10^{-4}	15.2
	1.750	6.58×10^{-3}	17.5
	2.250	1.79×10^{-4}	21.6
C-3-3 (60%)	1.125	8.33×10^{-4}	13.5
	1.250	1.67×10^{-4}	14.4
	1.375	7.81×10^{-5}	15.2
	1.500	7.35×10^{-4}	16.0
	1.625	1.25×10^{-4}	16.8
	1.750	4.17×10^{-4}	17.5
	1.937	3.75×10^{-3}	19.0
	2.250	2.08×10^{-4}	21.6
C-3-10 (60%)	1.125	5.00×10^{-4}	13.5
	1.250	1.67×10^{-4}	14.4
	1.375	1.25×10^{-4}	15.2
	1.500	4.17×10^{-3}	16.0
	1.625	1.25×10^{-3}	16.8
	2125	2.50×10^{-3}	20.4

TABLE 11.
(cont'd)

Specimen (Load Cycle)	Crack Length (in)	Crack Growth Rate (in/cyc)	K ($ksi\text{-}in^{\frac{1}{2}}$)
A-1-5 (70%)	1.125	1.25×10^{-3}	15.7
	1.250	2.08×10^{-3}	16.8
	1.375	2.50×10^{-3}	17.8
	1.625	8.33×10^{-3}	19.5
	2.000	9.38×10^{-3}	22.6
A-3-5 (70%)	1.125	2.50×10^{-3}	15.7
	1.375	1.39×10^{-3}	17.8
	1.500	7.35×10^{-4}	18.6
	1.750	3.57×10^{-3}	20.5
	2.125	9.38×10^{-3}	23.8
A-4-8 (70%)	1.125	1.04×10^{-3}	15.7
	1.250	1.56×10^{-3}	16.8
	1.375	3.12×10^{-3}	17.8
	1.500	2.08×10^{-3}	18.6
	1.750	8.33×10^{-3}	20.5
	2.000	8.33×10^{-3}	22.6
A-1-1 (80%)	1.500	5.55×10^{-3}	21.3
A-1-3 (80%)	1.125	2.50×10^{-3}	18.0
	1.312	3.75×10^{-3}	19.8
	2.000	1.38×10^{-2}	25.9
A-3-3 (80%)	1.125	1.25×10^{-3}	18.0
	1.312	2.34×10^{-3}	19.8
	1.812	1.00×10^{-2}	24.1

APPENDIX C.

SPECIMEN FABRICATION

The technique employed to fabricate the GRP plates from which specimens were to be cut was intended to approximate an actual production technique. The hand lay-up used no pressure or heat other than the manually-applied force of the men making the plates and the heat that developed from the exothermic curing process.

The chopped fiber, random mat glass ($1\frac{1}{2}$ oz/ft^2 - Stevens Fiberglass Co.) and the woven roving glass fabric (Style 779; 18 oz/yd^2; 9 strands per 2 inches warp, 7 strands per 2 inches fill - Stevens Fiberglass Co.) were cut from 38" wide rolls in sections 30" long and placed aside. A rigid wooden platform, 48" by 48", was covered with a sheet of mylar to prevent adhesion of the matrix to the wood. The amount of matrix required was determined largely by trial-and-error to be about 150% of the amount calculated to be necessary to provide a finished plate with a volume fraction of about 30%. The excess resin permitted work to progress at a quick enough pace so that the plate was not too far along in its cure before its completion.

The resin (number 4155 Laminac polyester resin - American Cyanamid Co.) was weighed in a five-gallon container. Methyl ethyl ketone peroxide (Specialty Chemicals Division; Reichold Chemicals, Inc.) was weighed in a separate container in an amount equal to 0.5% by weight of the resin and

then thoroughly mixed with the resin.

A generous amount of the activated resin was spread on the mylar-covered platform. A single layer of chopped mat was placed on the resin and more resin was poured over it. The resin was worked into the entire area of the glass mat using aluminum rollers. One layer of woven roving and one layer of random mat were then added and additional resin was worked into the entire area. The final six layers of glass were added in three steps in the same manner. The resin was always applied on the random mat to avoid spreading the strands of the woven roving when working the resin into the glass cloth. Firm pressure on the rollers insured adequate penetration of the resin and complete wetting of the glass fibers.

Another sheet of mylar was then placed on top of the uncured plate and steel shims, 0.185" thick, were laid parallel to all four sides. A steel pipe was placed across the plate and rested on the shims. Pressure was applied to the pipe by two men while rolling it across the plate to force out air and excess resin. The shims served to control plate thickness to achieve the desired volume fraction. The plate was then allowed to cure overnight and was removed the next day for eventual marking, cutting and machining.

Completed plates were marked and numbered for specimen preparation as shown in Figures 1a-c. The specimen layout provided 3/16" over final dimensions to allow for cutting

error and machining. A table saw with an installed diamond-impregnated blade was used to cut the specimen shapes from the plates. Final machining was accomplished using a router installed inverted in a Tensil-Kut table.

The shape for the dogbone specimens was obtained using a template developed experimentally and made by Kashihara (5) for a separate study. The shape development was based on photoelastic observations to eliminate stress concentrations. The final dogbone specimens were 10" long, 2" wide at the ends and were parallel-sided for a length of 1½" at the middle of the neck. Minimum width of the neck was 1½".

The index card specimens were drilled in a drill press with a ½" carbide-tipped bit. Notches 1½" long were cut using a 0.025" thick diamond-impregnated blade installed in a shaper.

For all specimens, the weak direction of the woven roving was parallel to the line of action of the applied force. One consequence of the hand lay-up technique was a moderate amount of variation in thickness from one location to another within a plate. Thickness measurements were taken of all specimens prior to testing and a global average of all specimen thicknesses (74 specimens) was used where required in the calculations. The global average thickness was 0.216 inch.

APPENDIX D.

DESCRIPTION OF APPARATUS

The apparatus used to obtain the basic data consisted of an Instron Model 1211 Dynamic Cycler, a circulating salt water presoak bath, and a specially-designed salt water containment system. Supplementary data were obtained using an Instron Universal Testing Machine and an Instron Universal Static/Dynamic Testing Instrument Model 1250.

All fatigue testing was performed on an Instron Model 1211 Dynamic Cycler which is a self-contained testing instrument capable of automatically maintaining a preset fatigue load cycle on an installed specimen. The machine applies a sinusoidal load cycle in either tension-only or tension-compression. The mean load must be preset but the operator is free to choose the other parameter to control in the load cycle. When a notched specimen, in which a crack grows over an interval of many cycles, is used or when the specimen is made of a material that undergoes significant plastic deformation before complete failure, the load is held constant by an increase in the stroke of the ram to which the lower grip assembly is attached. Control of the stroke can be maintained manually or automatically. The frequency of load reversals can be controlled between 4 and 35 Hz. Loads are read as percentages of full range with full load ranges of 2,000, 4,000, and 10,000 pounds available. Total number of cycles applied to a specimen are displayed on a

frequency counter which advances one digit for every ten cycles.

It is a characteristic of this machine that an interval of about 100 cycles (at 6 Hz) is required for the machine to build up to the desired load cycle after the AUTO button is depressed. Similarly, when a specimen fractures, the machine stops itself by driving the ram to its lower limit but continues to count cycles during this process. These factors were probably responsible for some inaccuracies in the data although careful attention was paid at the beginning and end of testing each specimen. Figure 3 shows the build-up, running and drive-down portions of the load cycle. The machine is shown in Figures 4a - d and the gripping assemblies are shown in Figures 5a - b.

The circulating salt water presoak bath was used to soak specimens for ten-day periods prior to testing in salt water. It was comprised of a copper tank 30" long, 15" high and 15" wide and an electrically-driven pump. Specimens were placed in a wooden rack weighted down with granite slabs. The tank was filled with salt water to a depth sufficient to cover the specimens entirely. The motor-driven pump was used to circulate the water (at room temperature) on an almost-continuous basis. The pump was stopped periodically to allow the motor to cool down. Salt water was added only to compensate for minor amounts lost through evaporation. (See Figure 6.)

In order to permit testing in a salt water environment,

a specially-designed salt water containment system was built for installation on the Dynamic Cycler. The system consisted of a box made of 3/8" plexiglas, open at the top and holed at the bottom to accept the grip holder that threaded into the ram of the Dynamic Cycler. Watertightness was maintained at the hole by using a 1-3/4" rubber O-ring and a 5" diameter custom-made retaining nut. Rigid, watertight construction of the box was achieved by drilling and tapping holes to accept 3/4", 10-24 zinc-plated screws. All mating surfaces were coated with RTV silicone rubber adhesive/sealant (General Electric Co.) prior to final tightening of the screws. (See Figure 7.)

APPENDIX E.

K-CALIBRATION

The primary experimental K-calibration method used was that suggested by Irwin and Kies for the determination of strain energy release rate (7). Three index card specimens were chosen at random and were notched to a depth of one inch. Each specimen was pinned in an Instron Universal Testing Machine and loaded to about 200 pounds using a crosshead rate of 0.02 in/min and a chart speed of 2.0 in/min. The chart recorded load vs deflection between loading points. The notch length was then increased to one and one-eighth inch and the specimens were again loaded to 200 pounds. This procedure was continued with the notch length being increased by one-eighth inch between successive loadings until the notch length reached two and one-eighth inches at which time the notch increment was changed to one-fourth inch between loadings. When the notch length reached four and one-eighth inches, a crack began to grow at the end of the notch with the application of even the smallest load and no more data could be taken.

Using the chart records, the compliance of the specimen for each notch length was calculated as the inverse of the slope of the load-deflection curve;

$$C = \frac{\Delta l}{\Delta P} .$$

The values of C for the three specimens at each notch

length were then averaged and these values of C_{ave} were plotted as a function of the notch length, a (measured from the center of the pin holes). The resulting curve was used to graphically determine values of $\frac{\partial C}{\partial a}$ as shown in Figure 9.

These values of $\frac{\partial C}{\partial a}$ were then plotted against notch length, a, and a smooth curve was drawn through the points. (See Figure 10.) For the remaining calculations, values of $\frac{\partial C}{\partial a}$ were taken from the curve rather than using the values obtained directly from the graphical technique.

Evaluation of strain energy release rate within each fatigue loading cycle was achieved by inserting the value of the maximum load in the cycle into the Irwin-Kies relationship;

$$G = \tfrac{1}{2} \frac{P_{max}^2}{B} \frac{\partial C}{\partial a} \quad ,$$

where the values of $\frac{\partial C}{\partial a}$ were dictated by the observed values of crack length.

The stress intensity factor corresponding to each value of G was then found from;

$$K = \sqrt{GE} \quad ,$$

where E was determined experimentally as described in Appendix F.

Data from the Irwin-Kies K-calibration are presented in Table 3. Data from the boundary collocation K-calibration are presented in Table 4.

APPENDIX F.

YOUNG'S MODULUS DETERMINATION

The value of Young's Modulus for the composite was found experimentally from a simple tensile test. Two dogbone specimens, chosen at random, were each fitted with two SR-4 strain gages (BLH Electronics), one to measure longitudinal strain and the other to measure transverse strain. (Poisson's ratio for the material could thus be determined although it was not used.) The strain gages were connected to a Wheatstone Bridge circuit which, in turn, was connected to a Hewlitt-Packard 321 Dual Channel Carrier Amplifier-Recorder.

The specimens were inserted into an Instron Universal Testing Machine and loaded in tension to about 1800 pounds. The load curve was recorded on the Instron recording chart and the strain was recorded on the Hewlitt-Packard strip recorder. (The Hewlitt-Packard recorder actually gave an output of $\frac{\Delta R}{R}$ in the bridge circuit. Strain was computed by dividing $\frac{\Delta R}{R}$ by the gage factor for the strain gage - 2.0 in this case.) Stress was found by dividing load from the Instron chart by the cross-sectional area of the test piece at the location of the strain gage.

Young's Modulus for each of the two specimens was measured and computed independently from the other using Hooke's Law;

$$E = \frac{\sigma}{\epsilon} .$$

The two values thus obtained were averaged to get a single value of E for use in the calculations to find K. The average value was found to be $E = 1.95 \times 10^3$ ksi.